CASSIANO RODRIGUES DE OLIVEIRA

TERMODINÂMICA DE ADSORÇÃO DE COMPOSTOS FENÓLICOS E AZOCORANTES EM NANOTUBOS DE CARBONO

Tese apresentada à Universidade Federal de Viçosa, como parte das exigências do Programa de Pós-Graduação em Agroquímica, para obtenção do título *Doctor Scientiae*.

VIÇOSA
MINAS GERAIS – BRASIL
2012

Ficha catalográfica preparada pelo Setor de Catalogação e Classificação da Biblioteca UFV Campus de Rio Paranaíba

T
O48t
2012

Oliveira, Cassiano Rodrigues de. 1979-
Termodinâmica de adsorção de compostos fenólicos e azocorantes em nanotubos de carbono / Cassiano Rodrigues de Oliveira – Viçosa, MG, 2012.
x, 73 f.: il. ; 29 cm.

Orientador: Luiz Henrique Mendes da Silva
Tese (Doutorado) - Universidade Federal de Viçosa, 2012
Inclui bibliografia.

1. Termodinâmica de adsorção 2. Nanotubos de Carbono. I. Universidade Federal de Viçosa. II.Título.

CDD 22.ed. 541

CASSIANO RODRIGUES DE OLIVEIRA

TERMODINÂMICA DE ADSORÇÃO DE COMPOSTOS FENÓLICOS E AZOCORANTES EM NANOTUBOS DE CARBONO

Tese apresentada à Universidade Federal de Viçosa, como parte das exigências do Programa de Pós-Graduação em Agroquímica, para obtenção do título *Doctor Scientiae*.

APROVADA: 17 de dezembro de 2012.

Prof. Jairo Tronto (Coorientador)	Prof. Alvaro Vianna Novaes de Carvalho Teixeira
Prof. Marco Antonio Schiavon	Prof. Sukarno Olavo Ferreira

Prof. Luis Henrique Mendes da Silva
(Orientador)

A DEUS,
À MINHA ESPOSA SABRINA,
AO MEU FILHO CAIO.

AGRADECIMENTOS

À Universidade Federal de Viçosa e ao Departamento de Química, pela oportunidade de realizar este trabalho.

Ao professor Luis Henrique Mendes da Silva, pela orientação, incentivo, e amizade.

Aos professores Maria do Carmo Hespanhol da Silva e Jairo Tronto, pela disponibilidade em apoiar, pelas sugestões e críticas.

Aos professores Alvaro Vianna Novaes de Carvalho Teixeira, Marco Antonio Schiavon e Sukarno Olavo Ferreira pela colaboração no enriquecimento deste trabalho.

Ao professor Rodrigo Lassarotte Lavall pelo companheirismo e apoio no desenvolvimento deste trabalho.

Aos colegas do QUIVECOM, pelo convívio e colaboração, em especial a Igor Boggione, Aparecida Mageste e aos irmãos Gabriel Max e Guilherme Max pelo apoio.

À minha esposa Sabrina e ao meu filho Caio, que além do carinho, compreenderam a importância desta conquista, que é da nossa família, e não minha.

Ao Conselho Nacional de Desenvolvimento Científico e Tecnológico (CNPq), à Fundação de Amparo a Pesquisa do Estado de Minas Gerais (FAPEMIG) e ao Instituto Nacional de Ciências e Tecnologias Analíticas Avançadas (INCTAA) pelos aportes financeiros para a realização deste trabalho.

BIOGRAFIA

CASSIANO RODRIGUES DE OLIVEIRA, filho de Antônio de Oliveira e de Climene Rodrigues de Oliveira, nasceu no dia 07 de fevereiro de 1979, em Cataguases – MG.

Em março de 1997, iniciou o curso de Química na universidade federal de Viçosa, diplomando-se em agosto de 2001, como Bacharel e Licenciado em Química.

Desenvolveu trabalhos como estudante de iniciação científica, no período de agosto de 1998 a julho de 2000, tendo como orientadora a Profª Mayura Marques Magalhães Rubinger, no Departamento de Química da Universidade Federal de Viçosa.

Desenvolveu trabalhos como estudante estagiário de agosto de 2000 a julho de 2001, tendo como orientador o Prof. Cláudio Mudado Silva, no Laboratório de Celulose e Papel do Departamento de Engenharia Florestal da Universidade Federal de Viçosa.

Em agosto de 2001, iniciou o Programa de Pós-Graduação em Ciência Florestal, a nível de Mestrado, obtendo o título de *Magister Scientiae* em agosto de 2003.

Matriculou-se em agosto de 2003 no Programa de Pós-Graduação em Ciência Florestal, nível de Doutorado.

No período de abril a agosto de 2004 foi professor substituto pelo Departamento de Química da Universidade Federal de Viçosa.

Em setembro de 2004, saiu do Programa de Pós-Graduação em Ciência Florestal e assumiu o cargo de Assistente Técnico da Gerência de Controle Técnico na empresa Veracel Celulose S.A. Ainda na mesma empresa, em julho de 2007, foi promovido ao cargo de Coordenador de Laboratório dentro da mesma Gerência.

Em março de 2010 assumiu o cargo de Professor Assistente I, na área de Química Analítica, pela Universidade Federal de Viçosa – Campus de Rio Paranaíba.

Em agosto de 2010, iniciou o Programa de Pós-Graduação em Agroquímica, nível de Doutorado, no Departamento de Química da Universidade Federal de Viçosa.

Tendo cumprido todas as exigências para a obtenção do título do *Doctor Scientiae*, defendeu tese em dezembro de 2012.

SUMÁRIO

LISTA DE FIGURAS

Artigo: Adsorption thermodynamics of phenolic compounds on multi-walled carbon nanotubes: a microcalorimetric approach

Artigo: Surface heterogeneity effect on azodyes adsorption onto multiwalled carbon nanotubes

LISTA DE TABELAS

Artigo: Adsorption thermodynamics of phenolic compounds on multi-walled carbon nanotubes: a microcalorimetric approach

Artigo: Surface heterogeneity effect on azodyes adsorption onto multiwalled carbon nanotubes

LISTA DE ABREVIATURAS

Introdução

CNTs	Nanotubos de carbono
SWCNT	Nanotubos de carbono de parede simples
MWCNT	Nanotubos de carbono de parede múltipla
CVD	Deposição química de vapor
AC	Carvão ativado
ICs	Canais intersticiais
$\Delta_{ads}H$	Variação de entalpia de adsorção

Artigo: Adsorption thermodynamics of phenolic compounds on multi-walled carbon nanotubes: a microcalorimetric approach

$\Delta_{ads}G^{o}$	Standard adsorption change free energy
PhCs	Phenolic compounds
ITC	Isothermal titration calorimetry
QUIVECOM	Química Verde Coloidal e Macromolecular
UFMG	Universidade Federal de Minas Gerais
SEM	Scanning Electron Microscopy
TEM	Transmission Electron Microscopy
PH	Phenol
MP	2-methylphenol
CP	4-chlorophenol
UV/Vis	Ultraviolet/visible
TG ou TGA	Thermogravimetric analysis
BET	Brunauer-Emmett-Teller method
DTG	Differential thermogravimetric analysis
HNO_3	Nitric acid
XPS	X-rays photoelectron spectroscopy
$\Delta_{ads}S^{o}$	Standard entropy change of adsorption

Artigo: Surface heterogeneity effect on azodyes adsorption onto multiwalled carbon nanotubes

AY	Acid yellow 42
AB	Acid black 210
AG	Acid green 68:1
AD	Azo dyes
MW	Molecular weight
H_2O_2	Hydrogen peroxide
NaCl	Sodium Chloride

RESUMO

OLIVEIRA, Cassiano Rodrigues de, D.Sc., Universidade Federal de Viçosa, Dezembro de 2012. **Termodinâmica de adsorção de compostos fenólicos e azocorantes em nanotubos de carbono.** Orientador: Luis Henrique Mendes da Silva. Coorientadores: Jairo Tronto e Maria do Carmo Hespanhol da Silva.

A termodinâmica de adsorção de compostos fenólicos e azocorantes em nanotubos de carbono de paredes múltiplas (MWCNT) foi avaliada por microcalorimetria de titulação isotérmica. As isotermas dos fenóis apresentaram tendências não-lineares e os modelos de isotermas de Langmuir e Freundlich ajustaram-se aos dados experimentais. A capacidade de adsorção máxima mostra que a ordem de adsorção é: fenol < 4-clorofenol < 2-metilfenol. Os valores de variação de energia livre de Gibbs padrão de adsorção ($\Delta_{ads}G^{o}$), variação de entalpia padrão de adsorção ($\Delta_{ads}H°$) e de variação de entropia padrão de adsorção ($\Delta_{ads}S°$) na adsorção dos fenóis em MWCNT mostraram que o processo é termodinamicamente espontâneo com ordem de espontaneidade de: fenol < 2-metilfenol < 4-clorofenol. Os resultados de microcalorimetria mostraram que os três processos são entalpicamente dirigidos e, os valores de $\Delta_{ads}H$ são da ordem daqueles atribuídos a interações de ligação de hidrogênio. O efeito de indução, causado pela presença de grupos funcionais (CH_3, H e Cl) em 2-metilfenol, fenol e 4-clorofenol, respectivamente, proporciona diferentes interações dos grupos funcionais oxigenados na superfície dos MWCNT através das hidroxilas (OH) fenólicas e efeitos de ressonância, resultando em valores distintos de $\Delta_{ads}H$. A adsorção dos azocorantes acid yellow 42 (AY), acid black 210 (AB) e acid green 68:1 (AG) em MWCNT apresentou isotermas não-lineares às quais o modelo de isoterma de Langmuir se ajusta e a ordem de adsorção é AG < AB < AY. A adsorção de todos os azocorantes em MWCNT foi termodinamicamente espontânea e as propriedades termodinâmicas estimadas a partir da aproximação de van't Hoff mostraram que o processo é endotérmico e entropicamente dirigido. A adsorção dos azocorantes em MWCNT mostrou-se diretamente proporcional à força iônica do meio enquanto a adsorção AY em MWCNT sofreu redução com a oxidação da superfície dos nanotubos de carbono. Estas observações sugerem que a natureza da superfície dos MWCNT seja heterogênea. As propriedades termodinâmicas obtidas pela microcalorimetria mostraram que, contradizendo os dados obtidos pela aproximação de van't Hoff, a natureza da adsorção em MWCNT é exotérmica para os três azocorantes. Além disso, a adsorção de AB e AG é entalpicamente dirigida, enquanto que para a adsorção de AY, tanto $\Delta_{ads}H°$

quanto $\Delta_{ads}S°$ contribuem para a espontaneidade do processo. Interações eletrostáticas e de forças de dispersão π-π podem ocorrer simultaneamente, explicando o mecanismo geral da adsorção, e a intensidade dessas interações depende da estrutura química do azocorante. Este trabalho mostra, pela primeira vez, que a técnica de microcalorimetria descreve a heterogeneidade da superfície dos MWCNT, evidenciando que os diferentes sítios de adsorção da superfície dos MWCNT interagem com os adsorvatos de maneiras distintas, dependendo da estrutura química do composto adsorvido.

ABSTRACT

OLIVEIRA, Cassiano Rodrigues de, D.Sc., Universidade Federal de Viçosa, December, 2012. **Thermodynamics of adsorption of phenolic compounds and azo dyes onto carbon nanotubes.** Adviser: Luis Henrique Mendes da Silva. Co-advisers: Jairo Tronto and Maria do Carmo Hespanhol da Silva

The thermodynamics of adsorption of phenolic compounds and azo dyes onto multi-walled carbon nanotubes (MWCNT) was evaluated by isothermal titration calorimetry (ITC). The adsorption isotherms of phenolic compounds presented non-linearity and good fitness of the Langmuir and Freundlich models to experimental data. The maximum adsorption capacity of phenols followed the order: phenol < 4-chlorophenol < 2-methylphenol. The changes of standard Gibbs free energy of adsorption ($\Delta_{ads}G^{o}$), standard enthalpy of adsorption ($\Delta_{ads}H°$) and standard entropy of adsorption ($\Delta_{ads}S°$) were determined and the adsorption of all phenolic compounds was spontaneous, with the following order of the decrease of $\Delta_{ads}G^{o}$: phenol < 2-methylphenol < 4-chlorophenol. Microcalorimetric measurements revealed that phenolic compounds adsorption is enthalpically driven and values of $\Delta_{ads}H$ are on the magnitude of hydrogen bonds. Hydrogen bonds are supposed to be the driving force for the adsorption process of phenolic compounds onto MWCNT. The inductor effect, caused by the functional groups (CH_3, H and Cl) presented in 2-methylphenol, phenol and 4-chlorophenol, respectively, builds different interactions between oxygenated functional groups on the MWCNT surface and phenolic hydroxyls (OH) and the resonance effects can be the reasons for distinct values of $\Delta_{ads}H$. The adsorption of acid yellow 42 (AY), acid black 210 (AB) and acid green 68:1 (AG) onto MWCNT presented isotherms with non-linear shapes, with good fitness of Langmuir model and following the order of adsorption: AG < AB < AY. The adsorption of all azo dyes onto MWNCT was spontaneous, endothermic and entropically driven, according to values of $\Delta_{ads}H°$ and $\Delta_{ads}S°$ estimated from van't Hoff approximation. The amount of azo dyes adsorbed increased proportionally with ionic strength and adsorption of AY onto MWCNT decreased when the surface of the carbon nanotubes is oxidized. These observations suggest a heterogeneous surface on MWCNT. The thermodynamic properties obtained by isothermal titration calorimetry differ from those estimated by van't Hoff approximation, and show that the adsorption of azo dyes onto MWCNT is an exothermic process. The adsorption of AB, AG and AY is enthalpically driven with $\Delta_{ads}S°$ influence on the spontaneity of AY adsorption process. Electrostatic interactions

and π-π dispersion forces may occur simultaneously in order to explain the general mechanism of azo dyes adsorption and the intensity of these interactions are dependent of the chemical structure of the azo dye. This work shows, for the first time, that the microcalorimetry describes the surface heterogeneity of MWCNT and, proves that the different sites of adsorption on the MWCNT surface interact distinctly with the molecules of the adsorbates, with intensities of interaction dependent of the chemical structure of the adsorbed compound.

1. INTRODUÇÃO

1.1. Nanotubos de Carbono

Nanoestruturas à base de carbono representam uma das classes de nanopartículas mais investigadas atualmente. Dentre elas destacam-se os nanotubos de carbono (CNT), pelas suas características físico-químicas singulares que despertam interesse desde sua divulgação por Iijima em 1991 [1]. Existem dois tipos básicos de CNT: nanotubos de carbono de parede simples (SWCNT) e nanotubos de carbono de paredes múltiplas (MWCNT) (Figura 1).

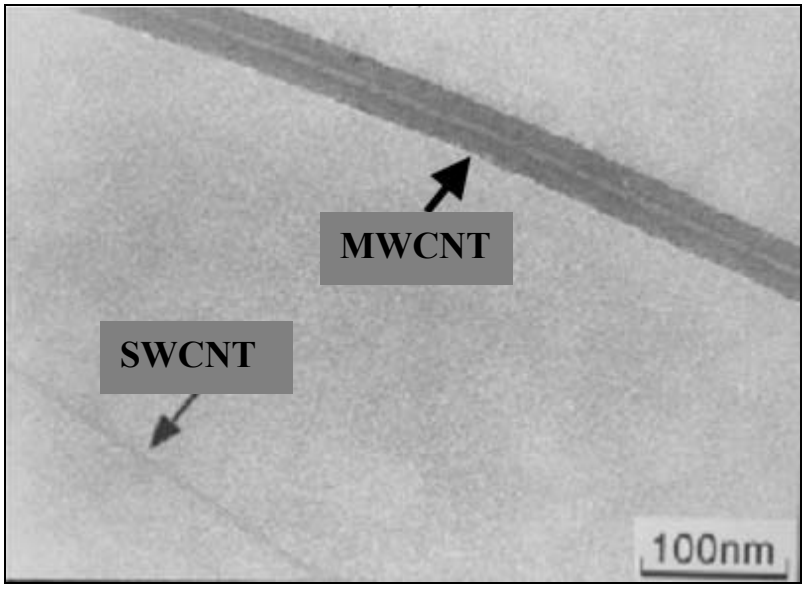

Figura 1 – Imagens de microscopia eletrônica mostrando nanotubos de carbono: SWCNT e MWCNT [2].

O SWCNT pode ser considerado como uma folha única de grafeno enrolada ao longo de um eixo característico na forma de cilindro. A força motriz para a formação de nanoestruturas fechadas de carbono tem sido atribuída à instabilidade do grafite em dimensões de poucos nanômetros, provocada pela alta energia das ligações erráticas – valência não preenchida - em átomos periféricos ou radicais livres imobilizados (*dangling bonds*) [5].

Esse enrolamento pode ocorrer de diferentes formas, originando nanotubos com propriedades distintas: “zigzag”, “armchair” e “quiral” (Figura 2) [3]. As formas de

enrolamento devem ser feitas de maneira que as ligações erráticas presentes nas extremidades da folha de grafeno possam ser coincidentes. Qualquer ligação com deslocamento translacional ao longo das extremidades, antes da conexão entre as ligações erráticas, resulta em diferentes orientações na rede com respeito a um eixo arbitrário do tubo. Desta forma, em uma estrutura generalizada do nanotubo, na superfície curva do tubo as redes hexagonais dos átomos de carbono se enrolam em uma forma helicoidal [5].

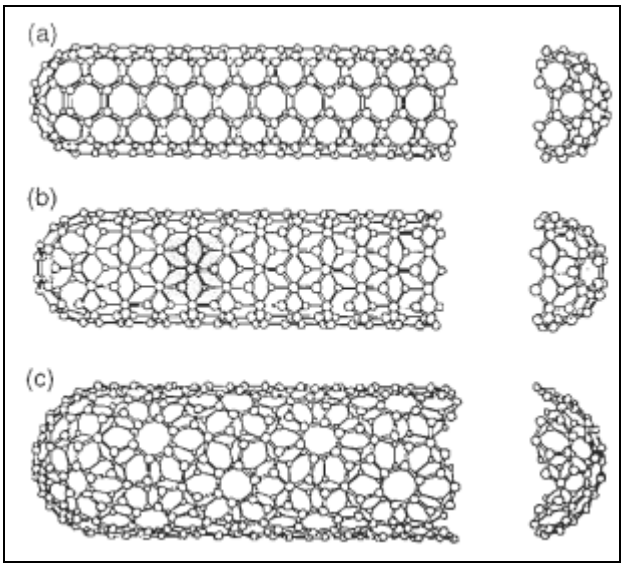

Figura 2 – Configurações helicoidais de um CNT: (a) "armchair"; (b) "zigzag"; (c) "quiral" [41].

O MWCNT é formado por vários cilindros de grafeno enrolados de forma concêntrica com distâncias interplanares de 0,34-0,36 nm e diâmetro externo de 2-25 nm [3]. Tanto SWCNT quanto MWCNT são produzidos basicamente por três técnicas: descarga por arco, ablação por laser e deposição química de vapor (CVD). A descarga por arco e a ablação por laser fundamentam-se na condensação de átomos de carbono gerados pela evaporação (sublimação) a partir de um precursor sólido, geralmente, grafite de alta pureza. A temperatura de evaporação envolvida aproxima-se da temperatura de fusão do grafite (3000-4000 ºC). O método CVD tem por princípio a decomposição de gases (ou vapores) precursores contendo átomos de carbono, geralmente, um hidrocarboneto, sobre um metal catalisador. A decomposição realiza-se, em geral, em temperaturas abaixo de 1000 ºC [4]. Todas as técnicas produzem misturas de nanotubos de diferentes tipos, diâmetros e comprimentos, juntamente com

impurezas, principalmente carbono amorfo, grafite e partículas metálicas dos catalisadores [5,6].

1.2. Propriedades Adsortivas e Modificação de Superfície de Nanotubos de Carbono

Dentre as várias aplicações dos CNT, destacamos a adsorção de compostos orgânicos [7-26]. As razões que favorecem a natureza adsorvente dos CNTs são: superfície inerte para adsorção química, alta área superficial específica, estrutura em escala atômica mais bem definida e uniforme - em comparação com carvão ativado (AC). Outros fatores que influenciam sua capacidade adsortiva são: sítios de adsorção específicos, estrutura porosa e tubular, baixa densidade, e interações com espécies poluentes [7].

A literatura possui vários estudos de comparação da capacidade de adsorção de CNT e outros materiais de carbono. Como exemplo, citamos o trabalho recente de Carabineiro *et al.* [42] que mostraram que a capacidade máxima de adsorção do antibiótico ciprofloxacina é 2,25 maior nos CNT estudados, em comparação com carvão ativado (AC). Liao *et al.* [10] também realizaram estudo comparativo entre CNT e AC para o adsorvente o-clorofenol e verificaram que a adsorção em CNT foi de 3,47 vezes superior àquela apresentada pelo AC, em termos de mg adsorvato por m^2. Ghaedi *et al.*. [43], compararam CNT e AC para a adsorção de eriocromo cianina R e, pelos valores de capacidade de adsorção, os CNT foram 2,34 vezes mais eficientes que o AC.

Além da capacidade adsortiva, outro fator que justifica a aplicação dos CNT como adsorventes é o tempo de alcance do equilíbrio termodinâmico. Geralmente, o equilíbrio termodinâmico do processo de adsorção utilizando-se carvão ativado (o adsorvente mais comum) é alcançado em longos períodos de tempo [10, 16]. Entretanto o mesmo comportamento não é observado para a adsorção em CNT. De fato, Peng *et al.* [16] observaram que o processo de adsorção de 1,2-diclorobenzeno em CNT leva 40 min para atingir o equilíbrio. Liao *et al.* [15], avaliando a adsorção de resorcinol em MWCNT modificados com HNO_3 ou não, observaram que com apenas 1 min de agitação, a quantidade de moléculas adsorvidas alcança 60 % do total adsorvido quando em equilíbrio. Nos experimentos de adsorção, o tamanho médio dos poros e a área superficial específica do adsorvente são considerados fatores primordiais. Entretanto, a química da interface pode influenciar no processo adsortivo, pois a presença de grupos

funcionais altera as propriedades físico-químicas dos materiais carbonáceos [27] e a natureza de suas interações com os adsorvatos [13]. Para a cinética de adsorção, a estrutura diferenciada dos CNT em comparação com a estrutura porosa do AC pode justificar o curto período de tempo de alcance do equilíbrio termodinâmico dos CNT, já que no AC as moléculas de adsorvatos devem se mover a partir da interface externa para a interface mais interna nos poros para atingir o equilíbrio [16].

A química da interface pode sofrer a influência de vários fatores. O primeiro deles são os grupos de sítios de adsorção da superfície. Existem quatro possíveis sítios em feixes de SWCNT para a adsorção de diferentes moléculas: (i) "sítios internos" – o interior tubular dos nanotubos individuais (acessíveis somente se as pontas dos nanotubos estiverem abertas e livres); (ii) "canais intersticiais (ICs)" – presentes entre os nanotubos dos feixes; (iii) "cavidades" – presentes na periferia de um feixe de nanotubos e a superfície externa dos nanotubos mais expostos, onde dois tubos adjacentes paralelos se encontram; e (iv) "superfície externa" – a superfície curva de nanotubos individualizados fora dos feixes de nanotubos, mostrados na Figura 3 [7,28]. Para MWCNT, os espaços entre as paredes no interior dos MWCNT também podem interagir com moléculas de adsorvatos. Estudos de adsorção em CNT contaminados revelam outros dois sítios de adsorção: superfície externa recoberta com carbono amorfo em camadas com espessuras nanométricas; e carbono recoberto com partículas de catalisadores [28-30].

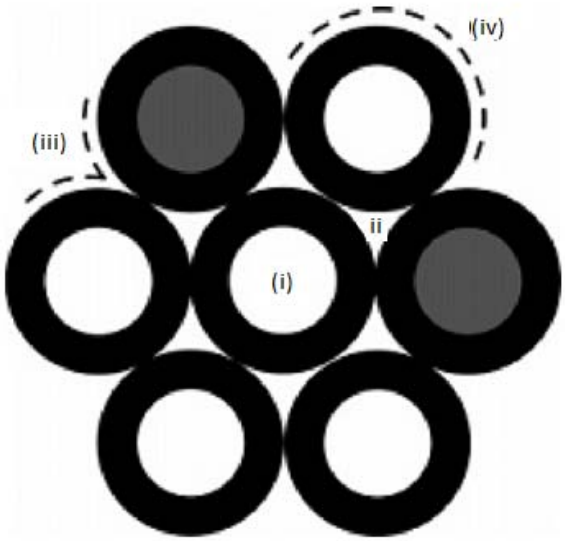

Figura 3 – Diferentes sítios de adsorção em um feixe homogêneo de SWCNT parcialmente abertos nas extremidades: (i) interno, (ii) canal intersticial; (iii) sítio de cavidade externa; e (iv) superfície externa [28].

O processo de adsorção sofre influência diferenciada de cada sítio. Na literatura, os sítios (iii) e (iv) possuem capacidade de adsorção; o sítio (ii) tem a capacidade de adsorção discutida por pesquisadores; pois seu tamanho depende do diâmetro dos CNT vizinhos [28]. Para o presente estudo, apenas os sítios (iii) e (iv) serão considerados. O sítio (i) não é considerado, pois, pelas suas dimensões permanece inacessível para os adsorvatos estudados. Como os sítio (i), sugere-se que o sítio (ii) também possui baixíssima acessibilidade dos adsorvatos devido à suas dimensões e logo, não é considerado neste estudo.

Após a síntese, os CNT podem apresentar as extremidades fechadas e a adsorção ocorre inicialmente nas cavidades entre tubos adjacentes dos feixes e, posteriormente, nos canais intersticiais, exclusivos para moléculas pequenas, como o CH_4.

O grau de pureza dos CNT determina os sítios que efetivamente participam do mecanismo de adsorção. Para CNT sintetizados e purificados, ou seja, com as extremidades abertas e livres, a adsorção ocorre primeiramente nas paredes internas dos nanotubos abertos, formando, em seguida, cadeias unidimensionais nas cavidades externas dos feixes. O processo se completa com o preenchimento dos sítios axiais no interior dos nanotubos.

Em termos de velocidade para se alcançar o equilíbrio, a adsorção ocorre mais rápida nos sítios externos (cavidades e superfícies mais externas) do que nos sítios internos (ICs e no interior do tubo) nas mesmas condições de experimento [7].

O segundo fator governante nos mecanismos de adsorção é a relação entre CNT abertos ou fechados. Os CNT abertos fornecem mais sítios de adsorção do que os fechados, tendo os primeiros maiores capacidades de adsorção. A disponibilização dos sítios internos, principalmente no processo de adsorção de gases monoatômicos, influencia diretamente no efeito citado acima. Este fator não influencia na adsorção dos adsorvatos estudados neste trabalho.

O terceiro fator é a presença de impurezas nos CNT, tais como carbono recoberto com partículas de catalisador, fuligem, e outras formas de carbono, que podem ser considerados adsorventes, “mascarando” as propriedades adsortivas dos CNT. Considerando o grau de pureza dos MWCNT testados em nossos experimentos, este fator foi desprezado.

Em quarto lugar, o teor de oxigênio nos CNT pode influenciar de forma positiva ou negativa a adsorção através de grupos funcionais presentes na interface (OH, C=O, e COOH) [7]. Alguns trabalhos mostram que CNT oxidados obtiveram aumento da área

superficial específica e da hidrofilicidade [10,17,31]. Entretanto, a introdução de grupos funcionais como principal fator que influencia na capacidade de adsorção ainda é discutida devido à presença de outros fatores decorrentes da funcionalização, tais como o aumento da área superficial específica. Por outro lado, a introdução de grupos funcionais *per se* atua na adsorção por tornar os CNT mais hidrofílicos [16], aumentando a resistência à difusão de moléculas orgânicas para os sítios de adsorção [7].

Por último, os átomos dopantes e os buracos formados na estrutura da cadeia de carbonos do nanotubo alteram as características da superfície, influenciando na adsorção [7].

1.3. Natureza das Interações de Compostos Orgânicos e Nanotubos de Carbono

Os CNT atuam como um material poroso flexível em relação a moléculas orgânicas. Em comparação com outros tipos de adsorventes tradicionalmente aplicados como sílica (colunas de cromatografia C_{18}), carvão ativado (AC) e peneiras moleculares de carbono, os CNT se apresentam como potenciais adsorventes para poluentes orgânicos.

Os fatores que afetam as interações de adsorção entre poluentes orgânicos e CNT podem ser agrupados em: propriedades dos CNT (tamanho, forma, áreas superficiais, volume e diâmetro médios dos poros, morfologia, grupos funcionais, impurezas), propriedades dos poluentes orgânicos (hidrofobicidade, polarizabilidade eletrônica, polaridade, tamanho, grupos funcionais), e condições ambientais (pH, força iônica) [7].

De acordo com os fatores estudados, as interações podem ser hidrofóbicas, forças de dispersão π-π, interações eletrostáticas e ligações de hidrogênio.

De forma generalizada, quando um composto orgânico é adicionado em água, as interações podem ser de natureza hidrofóbica ou hidrofílica. Para um soluto hidrofóbico, ao invés da dissolução, como acontece em solutos hidrofílicos, ocorrerá a formação de uma cela ou gaiola de moléculas de água ao redor da(s) molécula(s) hidrofóbica(s), isolando-a(s). Neste processo, há a redução da entropia das moléculas de água devido à formação de quatro ligações de hidrogênio coordenadas, de forma mais ordenada do que no seio da fase [44]. Logo, a redução de entropia decorrente deste

efeito é diferenciada de soluto para soluto, influenciando mais ou menos na capacidade adsortiva dos CNT.

Para a adsorção de compostos aromáticos em CNT, as forças de dispersão π-π são indicadas como as principais responsáveis pela adsorção [8,10,20,32,33] As interações do tipo π-π são de natureza atrativa e não-covalente entre anéis aromáticos e dependem do tamanho e da forma do sistema aromático e dos substituintes das moléculas. No caso da adsorção de compostos aromáticos em CNT, há variação na capacidade adsortiva de acordo com a estrutura molecular de cada adsorvato estudado. A literatura evidenciou a existência de tais interações [34,35], e o primeiro e mais aceito modelo prevê a influência de grupos substituintes do anel aromático dos adsorvatos na capacidade de adsorção [36]. De acordo com o modelo, tanto grupos substituintes doadores de elétrons (ex.: NH_2 e OH) quanto grupos retiradores de elétrons (ex.: NO_2 e Cl) podem promover a adsorção de compostos aromáticos monossubstituídos em CNT de maneira diferenciada em relação às moléculas aromáticas sem grupos substituintes.

A interação predominante depende dos diferentes tipos de compostos orgânicos, sendo que, a predição da adsorção destes compostos com os CNT não pode ser diretamente correlacionada. Desta maneira, a natureza das interações existentes no processo de adsorção entre certo(s) adsorvato(s) e os CNT é, a princípio, singular, não podendo ser prevista, mas sim determinada experimentalmente.

Alguns trabalhos têm explorado a natureza das interações de compostos aromáticos e CNT por meio de combinações de diferentes técnicas analíticas, tais como espectroscopias de infravermelho, Raman e de difração de raios-X [17-19,22]. Outros estudos explicam o processo adsortivo por meio de propriedades termodinâmicas determinadas indiretamente, levando-se em consideração uma superfície homogênea nos CNT [16-19,31,37]. Entretanto, não há relatos na literatura da descrição da natureza da superfície dos CNT por meio da técnica de microcalorimetria de titulação isotérmica, sendo este trabalho, pioneiro.

1.4. Descrição da Interface Heterogênea de Nanotubos de Carbono Via Microcalorimetria

A adsorção em fase líquida é um fenômeno complexo que necessita, para melhor entendimento, de métodos capazes de caracterizar a superfície em termos de área superficial, porosidade, natureza e energia dos sítios de adsorção [38]. A

microcalorimetria é capaz de elucidar a natureza química da superfície dos CNTs e sua contribuição ao processo adsortivo, pela adoção de moléculas-modelo como adsorvatos. Essa compreensão é obtida pela correlação dos valores de variação de entalpia de adsorção ($\Delta_{ads}H$) em função da quantidade adsorvida do adsorvato (Γ). O perfil da curva obtida determina: a natureza do processo (endotérmico ou exotérmico), a magnitude da energia de adsorção – que define o tipo de interação e a natureza da superfície (homogênea ou heterogênea).

A técnica termodinâmica utilizada neste trabalho é a calorimetria de titulação isotérmica, aplicada no monitoramento de qualquer reação química iniciada pela adição de um componente ligante, muito útil na caracterização de interações biomoleculares. Quando substâncias se ligam ou interagem, energia na forma de calor é liberada ou absorvida. A medida desta energia permite a determinação precisa de constantes de ligação (K), estequiometria de reação (n), variação de entalpia (ΔH) e variação de entropia (ΔS), por meio dos quais é possível obter um perfil termodinâmico completo das interações através de um único experimento.

Na ITC, uma seringa contendo uma solução de um componente "A" é titulada no interior de uma cela de reação contendo uma solução de um componente "B" a temperatura constante. Quando o componente "A" é injetado na cela de reação, os dois componentes interagem, e a energia a forma de calor é liberada ou absorvida na proporção direta da quantidade de ligações ou interações. À medida que o componente "B" na cela de reação é saturado com o componente "A", após sucessivas injeções, o sinal de energia na forma de calor diminui até que somente o sinal de fundo ("background") de diluição é observado.

Para as interações de adsorvatos em uma superfície homogênea (ex.: proteína em AC), as interações entre os componentes são da mesma natureza, logo, o valor de $\Delta_{ads}H$ em cada injeção é constante, sendo o perfil de curva linear. Por outro lado, um perfil não-linear é próprio de interações de naturezas distintas à medida que o componente "B" é saturado com o componente "A". No caso da adsorção de compostos fenólicos e azocorantes em MWCNT, este perfil de curva é observado e demonstra a heterogeneidade da superfície dos MWCNT.

Alguns estudos teóricos mostraram como compostos adsorvidos se comportam em CNT, mas poucos trabalhos experimentais focaram na adsorção de moléculas orgânicas em MWCNT e nos efeitos da heterogeneidade da superfície nestas interações. O estudo de Blanco-Martínez *et. al.* [38] mostra que a variação de entalpia de adsorção de compostos fenólicos monohidroxilados depende da posição da hidroxila substituinte

no anel aromático, focando na natureza dos adsorvatos. Em outro exemplo, um estudo sobre a interação de alguns vapores orgânicos não-aromáticos em CNTs com extremidades fechadas mostrou que a curvatura dos CNT pode afetar os valores de energia de adsorção [39]. Em trabalho mais recente, os autores concluem que moléculas orgânicas polares podem formar ligações de hidrogênio devido aos grupos funcionais da superfície dos CNT [40].

Algumas classes de compostos orgânicos, tais como fenóis e azocorantes (moléculas-modelo foram definidos para este estudo), são impactantes na carga poluidora de despejos industriais, sendo seu controle e monitoramento relevantes. Nos fenóis, a mudança dos grupos funcionais no anel aromático, bem como suas posições, podem alterar a intensidade ou natureza das interações dominantes na adsorção em MWCNT. Por outro lado, as estruturas com múltiplos anéis aromáticos dos azocorantes permitem verificar se estruturas complexas possuem semelhanças no mecanismo de adsorção.

De posse de informações obtidas pela adsorção de tais moléculas-modelo em CNT têm-se as seguintes ações potenciais:

- Conhecer a físico-química de adsorção para fenóis e azocorantes em MWCNT;
- Elucidar a natureza da superfície de MWCNT;
- Predizer o comportamento de classes de compostos em CNT;
- Aplicar nanoestruturas para detecção de analitos;
- Desenvolver tecnologias de adsorção e de tratamento [7,24,25].

2. OBJETIVOS

Os objetivos que motivam a realização deste trabalho são:

- Estudar a natureza das interações intermoleculares de moléculas-modelo (fenóis e azocorantes) e MWCNT;
- Determinar as forças motrizes de adsorção através dos parâmetros termodinâmicos $\Delta_{ads}H°$, $\Delta_{ads}S°$, $\Delta_{ads}G°$;
- Descrever a interface dos MWCNT via Calorimetria de Titulação Isotérmica.

3. MATERIAIS E MÉTODOS

3.1. Materiais

Os nanotubos de carbono (MWCNT) foram obtidos junto à empresa coreana CNT CO., LTD. Na classe dos fenóis, o fenol (C_6H_5OH), 2-metilfenol (C_7H_8OH) e 4-clorofenol (C_6H_5OHCl), adquiridos junto à Sigma-Aldrich, têm todos pureza superior a 99%. Os azocorantes, acid yellow 42 ($C_{32}H_{24}N_8Na_2O_8S_2$), acid black 210 ($C_{34}H_{25}K_2N_{11}O_{11}S_3$) e acid Green 68:1 ($C_{34}H_{25}N_9O_{13}S_3$) foram cedidos pela BASF do Brasil LTDA.

3.2. Métodos

3.2.1. Caracterização dos MWCNT

A caracterização dos MWCNT foi realizada utilizando-se as técnicas de microscopia eletrônica de varredura (SEM) e de transmissão (TEM), adsorção/dessorção de N_2 a 77K para determinação da área superficial (método BET) e termogravimetria (TG). Estas técnicas possibilitaram a confirmação dos dados obtidos junto ao fornecedor.

3.2.2. Funcionalização dos MWCNT

A funcionalização dos MWCNT foi realizada de acordo com procedimentos já publicados na literatura [17,45].

Misturou-se 100 mL de HNO_3 concentrado e 1 g de MWCNT, sob constante agitação, à temperatura ambiente por 24 horas. Os nanotubos obtidos neste procedimento foram chamados de MWCNT-acid.

Misturou-se 100 mL de H_2O_2 a 18 % e 1 g de MWCNT, sob constante agitação, à temperatura de 80 °C por 4 horas. Os nanotubos obtidos neste procedimento foram chamados de MWCNT-oxid.

Os adsorventes funcionalizados foram filtrados utilizando-se papel de filtro quantitativo, lavados com água destilada em abundância, secos e pulverizados.

3.2.3. Aquisição das isotermas de adsorção

As isotermas de adsorção foram obtidas a partir de experimentos de batelada e em duplicata, por meio de frascos de vidro para centrifugação de 40 mL fechados com tampas rosqueadas de "headspace". Uma medida exata de massa de MWCNT foi adicionada aos fracos juntamente com volume conhecido de solução de adsorvato em concentrações iniciais (C_0) pré-definidas de forma a garantir que uma isoterma de adsorção pudesse ser obtida. Os frascos contendo MWCNT e solução sofreram agitação e, em seguida, foram colocados verticalmente em um banho termostatizado, em temperatura pré-definida.

Após 24h - alcance do equilíbrio termodinâmico – os frascos foram centrifugados e uma alíquota do sobrenadante foi recolhida para análise em espectrofotometria de absorção molecular (UV-Vis), determinando-se, pela Lei de Beer, a concentração de equilíbrio adsorvato após adsorção (Ce). A partir desta determinação, obtém-se o valor da quantidade adsorvida através da equação (1) a seguir:

$$\Gamma = \left(\frac{C_0 - C_e}{m} \right) V \qquad (1)$$

em que Γ é a quantidade adsorvida de cada adsorvato em MWCNT (mg g^{-1}) após equilíbrio termodinâmico; C_0 é a concentração inicial (mg mL^{-1}); C_e é a concentração de equilíbrio (mg mL^{-1}); V é o volume da solução (mL) e m é a massa de MWCNT (g).

As isotermas de adsorção foram obtidas através da relação gráfica entre quantidade adsorvida (Γ) e concentração de equilíbrio (Ce).

Para o azocorantes, foram adquiridas isotermas testando-se a força iônica do meio em 0,1 e 0,01 mol NaCl L^{-1} e para o azocorante acid yellow 42 foram obtidas isotermas com os MWCNT modificados do item 3.2.2.

3.2.4. Determinação das propriedades termodinâmicas

3.2.4.1. Determinação de $\Delta_{ads}G°$

A variação da energia livre de Gibbs padrão de adsorção é definida por:

$$\Delta_{ads} G^o = -RT \ln K^o \quad (2)$$

em que K° é a constante de equilíbrio do processo de adsorção, R é a constante universal dos gases e T é a temperatura em Kelvin. Define-se como a constante de equilíbrio num processo de adsorção como a razão entre a atividade de um componente "i" na interface e a atividade deste mesmo componente em solução. Em concentrações do adsorvente em solução próximas de zero, o coeficiente de atividade aproxima-se da unidade, logo, a constante de equilíbrio é expressa por:

$$\ln K^o = \ln\left(\frac{a_i^{\text{int}}}{a_i^{sol}}\right) = \ln\left(\frac{C_i^{\text{int}}}{C_i^{sol}}\right), \text{ com } \frac{C_i^{\text{int}}}{C_i^{sol}} = \frac{\Gamma}{C_e} \quad (3)$$

3.2.4.2. Determinação de $\Delta_{ads}S°$

A variação de entropia padrão de adsorção é obtida a partir da equação fundamental de Gibbs-Helmholtz:

$$\Delta_{ads} G^o = \Delta_{ads} H^o - T\Delta_{ads} S^o \quad (4)$$

Neste caso, a determinação de $\Delta_{ads}H°$ permite-nos a obtenção de $\Delta_{ads}S°$ por diferença na equação (4).

3.2.4.3. Determinação de $\Delta_{ads}H°$

A variação de entalpia padrão de adsorção foi obtida via ITC para a adsorção de fenóis em MWCNT e, para a adsorção dos azocorantes em MWCNT aplicou-se ITC e a estimativa pela aproximação de van't Hoff.

A aproximação de van't Hoff pode ser obtida a partir da combinação das equações (4) e (2), como segue abaixo:

$$\ln K^o = -\frac{\Delta_{ads} H^o}{RT} + \frac{\Delta_{ads} S^o}{R} \quad (5)$$

Pela equação (5), o termo $\Delta_{ads}H°$ pode ser obtido a partir da inclinação da reta proveniente da regressão linear do gráfico de ln K° versus 1/T.

Em ITC, o termo $\Delta_{ads}H°$ é obtido a partir da extrapolação dos valores de Ce a zero, utilizando uma regressão exponencial em um gráfico de correlaciona $\Delta_{ads}H$ em função de Ce.

3.2.5. Ajuste de modelos de isotermas

Dois modelos foram ajustados aos dados experimentais: Langmuir e Freundlich. Estes modelos estão entre os mais aplicados na literatura para ajustes de isotermas [17,18].

A isoterma de Langmuir é concebida para um processo de adsorção em um sistema ideal, em que as moléculas de adsorvato se concentram na interface do adsorvente em sítios bem definidos, formando uma monocamada homogênea. Neste modelo, assume-se que cada sítio de adsorção adsorve apenas uma única molécula, e que a energia envolvida na adsorção de uma molécula de adsorvato é a mesma para todos os sítios da interface e que este conteúdo energético independe da presença ou não de outras moléculas nos sítios adjacentes, ou seja, não há interação entre moléculas adjacentes de adsorvato. A expressão (6) representa a equação matemática do modelo de Langmuir:

$$\Gamma = \frac{\Gamma_{\max} K_L C_e}{1 + K_L C_e} \qquad (6)$$

sendo C_e a concentração no equilíbrio do adsorvato em mg mL^{-1}, Γ a quantidade adsorvida do adsorvato em mg g^{-1}, K_L uma constante de Langmuir relacionada à afinidade dos sítios ligantes (energia de adsorção), e Γ_{max} (expressa em mg g^{-1}), uma constante de Langmuir relacionada com a máxima capacidade de adsorção em monocamada, que descreve a monocamada saturada de moléculas de soluto na interface (a capacidade de saturação teórica da monocamada), o que significa que adsorção posterior vai contribuir para um aumento da energia livre de Gibbs na interface, o que não é permitido.

O modelo da isoterma empírica de Freundlich preconiza a existência de uma interface heterogênea com diferentes sítios e, portanto, diferente energias de adsorção e

na possibilidade de formação de multicamadas. A expressão (7) representa a equação matemática do modelo de Freundlich:

$$\Gamma = K_F C_e^{1/n} \qquad (7)$$

Onde C_e e Γ foram descritos anteriormente, K_F (expressa em $mg^{(1-1/n)}\ mL^{(1/n)}\ g^{-1}$) e n são constantes de Freundlich que descrevem a capacidade de adsorção e a distribuição de energia dos sítios de adsorção assim como a magnitude da força predominante de adsorção, respectivamente. Os modelos de Langmuir e Freundlich podem ajustar os dados experimentais a partir da aplicação de suas formas linearizadas.

$$\frac{C_e}{\Gamma} = \frac{1}{\Gamma_{max}} C_e + \frac{1}{K_L \Gamma_{max}} \qquad (8)$$

$$\ln \Gamma = \ln K_F + \frac{1}{n} \ln C_e \qquad (9)$$

Os diagramas de $\frac{C_e}{\Gamma}$ x C_e e $ln\Gamma$ x lnC_e permitem calcular as constantes de Langmuir e Freundlich, respectivamente.

4. RESULTADOS E DISCUSSÃO

Neste item, apresenta-se um resumo dos principais resultados e discussões abordados nos artigos da Tese.

4.1. Caracterização dos MWCNT

A caracterização realizada nos MWCNT concorda com os resultados apresentados para TG, SEM, TEM e área superficial específica. Os MWCNT possuem pureza superior a 90%, comprimento variando de 1-25 μm e diâmetro variando de 10-40 nm. A área superficial específica BET é da ordem de 188 $m^2\ g^{-1}$.

4.2. Adsorção de fenóis em MWCNT

Os fenóis apresentaram isotermas de adsorção em MWCNT não lineares, em que os modelos de Langmuir e Freundlich se ajustaram. A ordem de adsorção foi de fenol < 4-clorofenol < 2-metilfenol. A termodinâmica de adsorção, com determinação de $\Delta_{ads}H°$ por ITC, mostrou que o processo é espontâneo e entalpicamente dirigido. Os valores de $\Delta_{ads}H°$ encontrados são de ordem de magnitude semelhante àqueles atribuídos a ligações de hidrogênio. O efeito de indução, causado pela presença de grupos funcionais (CH_3, H e Cl) em 2-metilfenol, fenol e 4-clorofenol, respectivamente, proporciona diferentes interações dos grupos funcionais oxigenados na superfície dos MWCNT através das hidroxilas (OH) fenólicas e efeitos de ressonância, resultando em valores distintos de $\Delta_{ads}H$.

4.3. Adsorção de azocorantes em MWCNT

A adsorção dos azocorantes acid yellow 42 (AY), acid black 210 (AB) e acid green 68:1 (AG) em MWCNT apresentou isotermas não-lineares às quais o modelo de isoterma de Langmuir se ajusta e a ordem de adsorção é AG < AB < AY. A adsorção de todos os azocorantes em MWCNT foi termodinamicamente espontânea e as propriedades termodinâmicas estimadas a partir da aproximação de van't Hoff mostraram que o processo é endotérmico e entropicamente dirigido. A adsorção dos azocorantes em MWCNT mostrou-se diretamente proporcional à força iônica do meio enquanto a adsorção AY em MWCNT sofreu redução com a oxidação da superfície dos nanotubos de carbono. Estas observações sugerem que a natureza da superfície dos MWCNT seja heterogênea. As propriedades termodinâmicas obtidas pela microcalorimetria mostraram que, contradizendo os dados obtidos pela aproximação de van't Hoff, a natureza da adsorção em MWCNT é exotérmica para os três azocorantes. Além disso, a adsorção de AB e AG é entalpicamente dirigida, enquanto que para a adsorção de AY, tanto $\Delta_{ads}H°$ quanto $\Delta_{ads}S°$ contribuem para a espontaneidade do processo. Interações eletrostáticas e de forças de dispersão π-π podem ocorrer simultaneamente, explicando o mecanismo geral da adsorção, e a intensidade dessas interações depende da estrutura química do azocorante.

5. CONCLUSÕES GERAIS DO TRABALHO

Este trabalho mostra, pela primeira vez, que a técnica de microcalorimetria descreve a heterogeneidade da superfície dos MWCNT, evidenciando que os diferentes sítios de adsorção da superfície dos MWCNT interagem com os adsorvatos de maneiras distintas, dependendo da estrutura química do composto adsorvido.

Para as moléculas-modelo fenol, 2-metilfenol e 4-clorofenol, a adsorção em MWCNT é entalpicamente dirigida com possível formação de ligações de hidrogênio e interações π-π.

A adsorção dos azocorantes acid black 210 e acid green 68:1 em MWCNT é entalpicamente dirigida; enquanto o composto acid yellow 42 possui contribuições da entropia e da entalpia na adsorção em MWCNT, segundo a técnica de ITC.

A aproximação de van't Hoff oferece interpretação incompleta e errônea sobre a natureza das interações na adsorção dos azocorantes em MWCNT.

6. REFERÊNCIAS

1. Iijima, S., Helical microtubules of graphitic carbon. Nature, 354, 56–58, 1991.

2. Dresselhaus, M.S., Endo, M. Relation of carbon nanotubes to other carbon materials. In: Dresselhaus, M.S., Dresselhaus, G., Avouris, Ph. eds. Topics in Applied Physics 80: Carbon Nanotubes: Synthesis, Structure, Properties, and Applications, Berlin, Springer, p.11-28, 2001.

3. Dresselhaus, M.S., Avouris, P. Introduction to carbon materials research. In: Dresselhaus, M.S., Dresselhaus, G., Avouris, Ph. eds. Topics in Applied Physics 80: Carbon Nanotubes: Synthesis, Structure, Properties, and Applications, Berlin, Springer, p.1-9, 2001.

4. Ferreira, O.P. Nanotubos de carbono: preparação e caracterização. Monografia de Exame Geral de qualificação de Doutorado do Instituto de Química da UNICAMP. Campinas, 2003, p.1.

5. Ajayan, P.M. Nanotubes from carbon. Chem. Rev., 99, 1787-1799, 1999.

6. Terrones, M. Carbon nanotubes: synthesis and properties, electronic devices and other emerging applications. Int Mater Rev, 49, 325-377, 2004.

7. Ren, X., Chen, C., Nagatsu, M., Wang, X. Carbon nanotubes as adsorbents in environmental pollution management: A review. Chem. Eng. J., 170, 395–410, 2011.

8. Lin D., Xing B. Adsorption of phenolic compounds by carbon nanotubes: role of aromaticity and substitution of hydroxyl groups, Environ. Sci. Technol.42, 7254-7259, 2008.
9. Long R.Q., Yang R.T., Carbon nanotubes as superior sorbent for dioxin removal, J. Am. Chem. Soc.123, 2058–2059, 2001.
10. Liao Q., Sun J., Gao L., Adsorption of chlorophenols by multi-walled carbon nanotubes treated with HNO_3 and NH_3, Carbon 46, 553-555, 2008.
11. Chen G-C., Shan X-Q., Zhou Y-Q., Shen X., Huang H-L., Khan S.U., Adsorption kinetics, isotherms and thermodynamics of atrazine on surface oxidized multiwalled carbon nanotubes, J. Hazard. Mater.169, 912-918, 2009.
12. Diaz-Florez P.E., López-Urías F., Terrones M., Rangel-Mendez J.R., Simultaneous adsorption of Cd^{2+} and phenol on modified N-doped carbon nanotubes: experimental and DFT studies, J. Colloid Interf. Sci. 334, 124-131, 2009.
13. Franz M., Arafat H.A., Pinto N.G., Effect of chemical surface heterogeneity on the adsorption mechanism of dissolved aromatics on activated carbon, Carbon 38, 1807-1819, 2000.
14. Kuo C-Y., Comparison with as-grown and microwave modified carbon nanotubes to removal aqueous bisphenol A, Desalination 249, 976-982, 2009.
15. Liao Q., Sun J., Gao L., The adsorption of resorcinol from water using multi-walled carbon nanotubes, Colloid. Surface. A 312, 160-165, 2008.
16. Peng X., Li Y., Luan Z., Di Z., Wang H., Tian B., Jia Z., Adsorption of 1,2-dichlorobenzene from water to carbon nanotubes, Chem. Phys. Lett. 376, 154-158, 2003.
17. Salam M.S., Burk R.C., Thermodynamics of pentachlorophenol adsorption from aqueous solutions by oxidized multi-walled carbon nanotubes, Appl. Surf. Sci. 255, 1975-1981, 2008.
18. Shen, X-E, Shan, X-Q, Dong, D-M, Hua, X-Y, Owens, G. Kinetics and thermodynamics of sorption of nitroaromatic compounds to as-grown and oxidized multiwalled carbon nanotubes, J. Colloid. Interf. Sci., 330, 1–8, 2009.
19. Sheng G.D., Shao D.D., Ren X.M., Wang X.Q., Li J.X., Chen Y.X., Wang X.K., Kinetics and thermodynamics of adsorption of ionizable aromatic compounds from aqueous solutions by as-prepared and oxidized multiwalled carbon nanotubes, J. Hazard. Mater., 178, 505-516, 2010.
20. Yang K., Wu W., Jing Q., Zhu Z., Aqueous adsorption of aniline, phenol, and their substitutes by multi-walled carbon nanotubes, Environ. Sci. Technol., 42, 7931–7936,

2008.
21. Yao Y., Xu F., Chen M., Xu Z., Zhu Z. Adsorption behavior of methylene blue on carbon nanotubes. Bioresource Technol, 101, 3040–3046, 2010.
22. Gong J.L., Wang B., Zeng G.M., Yang C.P., Niu C.G., Niu Q.Y., Zhou W.J., Liang Y. Removal of cationic dyes from aqueous solution using magnetic multi-wall carbon nanotube nanocomposite as adsorbent. J. Hazard Mater, 164, 1517–1522, 2009.
23. Kuo C.Y., Wu C.H., Wu J.Y. Adsorption of direct dyes from aqueous solutions by carbon nanotubes: Determination of equilibrium, kinetics and thermodynamics parameters. J. Colloid. Interf. Sci., 327, 308–315, 2008.
24. Mishra A.K., Arockiadoss T., Ramaprabhu S. Study of removal of azo dye by functionalized multi walled carbon nanotubes. Chem. Eng. J., 162, 1026–1034, 2010.
25. Wu C.H. Adsorption of reactive dye onto carbon nanotubes: Equilibrium, kinetics and thermodynamics. J. Hazard. Mater., 144, 93–100, 2007.
26. Shapour R., Mehrorang G., Kianoosh M. Multiwalled carbon nanotubes as efficient adsorbent for the removal of congo red. Fresen. Environ. Bull., 20(10), 2514-2520, 2011.
27. Ania C.O., Bandosz T.J., Surface chemistry of activated carbons and its characterization, In: Bandosz T.J. (Ed.), Activated carbon surfaces in environmental remediation, Oxford, Elsevier, 2006, pp. 159-230.
28. Agnihotri, S.; Rostam-Abadi, M.; Rood, M.J. Temporal changes in nitrogen adsorption properties of single-walled carbon nanotubes. Carbon, 42, 2699–2710, 2004.
29. Yang K., Xing B. Desorption of polycyclic aromatic hydrocarbons from carbon nanomaterials in water. Environ. Pollut., 145, 529–537, 2007.
30. Zhao J., Buldum A., Han J., Lu J.P. Gas molecule adsorption in carbon nanotubes and nanotube bundles. Nanotechnology, 13, 195-200, 2002.
31. Xie X., Gao L., Sun J. Thermodynamic study on aniline adsorption on chemical modified multi-walled carbon nanotubes. Colloid. Surface. A, 308, 54–59, 2007.
32. Du W., Zhao F., Zeng B. Novel multiwalled carbon nanotubes–polyaniline composite film coated platinum wire for headspace solid-phase microextraction and gas chromatographic determination of phenolic compounds. J. Chromatogr. A, 1216, 3751-3757, 2009.
33. Chen W., Duan L., Wang L., Zhu, D. Adsorption of hydroxyl- and amino-substituted aromatics to carbon nanotubes. Environ. Sci. Technol., 42, 6862–6868, 2008.

34. Sinnokrot M.O., Valeev E.F., Sherrill C.D. Estimates of the ab initio limit for pi-pi interactions: The benzene dimer. J. Am. Chem. Soc., 124, 10887–10893, 2002.
35. McGaughey, G.B.; Gagné, M.; Rappé, A.K. Pi-Stacking interactions. alive and well in proteins. J. Biol. Chem., 273, 15458–15463, 1998.
36. Hunter C.A., Sanders J.K.M. The nature of .pi.-.pi. interactions. J. Am. Chem. Soc. 112, 5525–5534, 1990.
37. Salam, M.A.; Mokhtar, M.; Basahel, S.N.; AL-Thabaiti, S.A.; Obaid, A.Y. Removal of chlorophenol from aqueous solutions by multi-walled carbon nanotubes: Kinetic and thermodynamic studies. J. Alloy. Compd., 500, 87–92, 2010.
38. Blanco-Martínez D.A., Giraldo L., Moreno-Piraján J.C. Immersion enthalpy of carbonaceous samples in aqueous solutions of monohydroxilated phenols. J. Therm. Anal. Calorim., 96, 853–857, 2009.
39. Wisniewki M., Rychlicki G., Arcimowicz A. Experimental and theoretical estimations of the polar force contributions to the heat of immersion of carbon nanotubes. Chem. Phys. Lett.,485, 331–334, 2010.
40. Castillejos E., Bachiller-Baeza B., Rodríguez-Ramos I., Guerrero-Ruiz A. An immersion calorimetry study of the interaction of organic compounds with carbon nanotube surfaces. Carbon, 50, 2731 –2740, 2012.
41. Dresselhaus M. S., Dresselhaus G., Saito R. Physics of carbon nanotubes. Carbon, 37, 883-891, 1995.
42. Carabineiro S.A.C., Thavorn-amorsri T., Pereira M. F. R., Serp P., Figueiredo J. L. Comparison between activated carbon, carbon xerogel and carbon nanotubes for the adsorption of the antibiotic ciprofloxacin. Catalysis Today, 186, 29-34, 2012.
43. Ghaedi M., Shokrollahi A., Hossainian H., Kokhdan S. N. Comparison of activated carbon and multiwalled carbon nanotubes for efficient removal of eriochrome cyanine R (ECR): kinetic, isotherm, and thermodynamic study of the removal process. J Chem Eng Data, 56, 3227-3235, 2011.
44. Junior, J. A. Efeito hidrofóbico de macromoléculas sobre a partição de cianocomplexos em sistemas aquosos bifásicos. Viçosa: Dissertação de mestrado, UFV, 2006.
45. El-Sheikh A. H. Effect of oxidation of activated carbon on its enrichment efficiency of metal ions: Comparison with oxidized and non-oxidized multi-walled carbon nanotubes. Talanta, 75, 127–134, 2008.

ARTIGO

Adsorption thermodynamics of phenolic compounds on multi-walled carbon nanotubes: a microcalorimetric approach

Abstract

The adsorption thermodynamics of phenol, 2-methylphenol and 4-chlorophenol onto pristine multi-walled carbon nanotubes (MWCNTs) was evaluated by measuring the following thermodynamic adsorption parameters: standard adsorption free energy change ($\Delta_{ads}G^o$), standard adsorption enthalpy change and standard adsorption entropy change. The adsorption of all phenolic compounds onto MWCNTs was a thermodynamically spontaneous process and the decrease in $\Delta_{ads}G^o$ follows the order phenol < 2-methylphenol < 4-chlorophenol. Isothermal Titration Calorimetry results show that the adsorption process is enthalpically driven and that MWCNT interfaces have sites with different interaction energies that allow specific interactions with phenolic compounds, not only π-π dispersion interactions.

1. Introduction

Among the more than 800 products based on nanoparticles or nanofibers, those formed by carbon materials, including fullerenes and carbon nanotubes, are the most numerous [1]. Carbon nanotubes (CNTs) possess unique physicochemical properties that have led to the research and the development of new products, advanced by the findings of Iijima in 1991 regarding the synthesis of the multi-walled carbon nanotubes (MWCNTs) [2]. Today, CNTs are employed in a wide range of applications, which include systems for energy conversion/power sources, sensors, supports for catalysts and biomedical materials [3,4]. In 2001, Long and Yang reported for the first time that CNTs could act as more efficient adsorbents for dioxin than activated carbon (AC) [5]. Adsorption is an established technique for removing organic pollutants from water [6] particularly using strategic materials as adsorbents [7]. Since 2001, several papers have been published seeking to evaluate the adsorption of organic pollutants by CNTs [3,6,8-17] with special attention paid to phenolic compounds (PhCs), which possess high toxicity to human health and the environment even at low concentrations [12,13]. In the

adsorption experiments, porosity and surface area of the adsorbent (especially of the carbon materials) were considered the primary factors influencing the phenomena. However, a knowledge of the surface chemistry is important, as even a small number of surface groups can exert a significant influence on the physicochemical properties of the carbon materials [18] and, therefore, on their adsorptive characteristics, including the nature of their interactions with the adsorbate molecules [10]. In the case of CNTs, according to N_2 adsorption data, the largest numbers of available spaces for adsorption are on the cylindrical external surface, not in the inner cavities or inner wall spacing [12,19]. Some studies reveal that the adsorption of phenolic compounds (PhCs) onto MWCNTs does not follow exactly the same mechanism observed in activated carbon. Evidence of this can be found in the fact that the total amount adsorbed reaches equilibrium within 30–40 min with MWCNTs, in comparison to 7–150 h with activated carbon [6,12,13]. CNTs are recognized as hydrophobic structures, and several works indicated that the π–π dispersion forces are responsible for the adsorption of aromatic compounds onto CNTs [3]. It is well known that some oxygen groups such as carbonyl, carboxylic and hydroxyl groups exist on the surface of CNTs [13], and recent studies demonstrate their influence on the adsorption process [6,11-15]. However, there is no agreement concerning the main driving force for the adsorption of phenol and phenolic derivatives onto the CNTs. Therefore, this study aims to evaluate the adsorption behavior of model molecules, formed with different functional groups that modulate the electron density of the phenol ring, onto MWCNTs. The study also contributes to the understanding of the nature of the interaction between nanotubes and PhCs as assessed by the thermodynamic properties, primarily using isothermal titration calorimetry.

2. Experimental

All adsorption experiments, ITC microcalorimetry and UV-Vis characterizations were performed in the laboratories of the QUIVECOM group at the Chemistry Department of the Federal University of Viçosa (UFV). Thermogravimetric analysis and N_2 adsorption experiments were performed at the Chemistry Department, Federal University of Minas Gerais (UFMG). The SEM and TEM images were obtained at the UFMG Microscopy Center.

2.1. Materials

The phenolic compounds (PhCs), phenol (PH), 2-methylphenol (MP) and 4-chlorophenol (CP), were purchased from Sigma-Aldrich, all with purity above 99.9%. Multi-walled carbon nanotubes, C_{TUBE} 100 MWCNTs, were purchased from CNT CO., LTD., Korea. Technical specifications for the MWCNTs were supplied by the manufacturer (average diameter: 10–40 nm; length: 1–25 μm; purity: 93 wt% min.; contaminants: 7 wt% max.; bulk density: 0.03–0.06 g cm^{-3}; specific surface area: 150–250 $m^2 g^{-1}$).

2.2. Adsorption Experiments

Adsorption isotherms were carried out in duplicate by mixing solutions (20 mL) containing various concentrations of adsorbates with 15 mg of MWCNT, except for the phenol solutions, in which 50 mg of MWCNT were used. All experiments were performed in 40-mL glass centrifuge tubes sealed with headspace screw caps. Initial concentrations were chosen to cover a complete spectrum of isotherm adsorption behavior. The tubes were shaken manually for 10 minutes in the dark to guarantee complete contact between the MWCNTs and the dissolved phenolic compound. After shaking, all tubes were placed vertically in a thermostatically controlled bath at 298.15 K in the absence of light. After reaching thermodynamic equilibrium, samples were taken from the adsorption tubes to determine the PhC concentration in the supernatants. Separation of the MWCNTs and the supernatants was achieved by centrifugation. The collected aliquots were then properly diluted to ensure that the absorbance readings in the UV/Vis spectrometer obeyed Beer's Law. PhC concentrations in the supernatants (equilibrium concentrations − C_e) were determined after 24 h, 120 h and 168 h of thermodynamic equilibrium. Blank experiments were carried out using the same experimental procedure without MWCNTs to examine the potential sorption of PhCs onto the glass tubes. The results indicated that such losses were negligible. Therefore, the amounts of PhCs adsorbed by the MWCNTs were directly calculated from difference between the initial and final equilibrium concentrations as follows:

$$\Gamma = \left(\frac{C_0 - C_e}{m} \right) V \tag{1}$$

in which Γ is the amount of each PhC adsorbed by the MWCNTs (mg g^{-1}) after thermodynamic equilibrium; C_0 is the initial concentration (mg mL^{-1}); C_e is the equilibrium concentration (mg mL^{-1}); V is the solution volume (mL); and m is mass of the MWCNTs (g).

The adsorbates were dissolved in distilled water, and the final concentrations were limited to <50% of their water solubility to guarantee complete dissolution. According to the literature, there is no considerable difference in the adsorption of PhCs on CNTs at pH values lower than the pK_a for each compound [12,17]. Therefore, the adsorption experiments were accomplished at the pH of distillate water at which PhC is in its non-dissociated form.

2.3. Characterization

N_2 adsorption: The specific surface area of the MWCNT was determined from the N_2 adsorption/desorption isotherms obtained in an automated gas sorption system, AUTOSORB-1 ASIAG (QUANTACHROME INSTRUMENTS), using the Brunauer-Emmett-Teller (BET) method.

Thermogravimetric Analysis (TG): Thermogravimetric measurements were carried out using a TA INSTRUMENTS SDT 2960 simultaneous TG/DTG at 5 °C min^{-1} in a dry airflow of 100 mL min^{-1} between 25 and 1000 °C in an alumina crucible.

Scanning Electron Microscopy: Scanning electron microscopy (SEM) was performed with a Quanta 200 FEG (FEI) scanning microscope. The carbon nanotube sample was placed on conductive carbon tape and covered with a thin gold layer (~10 nm) for better visualization, improving contrast.

Transmission Electron Microscopy: Transmission electron microscopy (TEM) was carried out with a Tecnai G-20 (FEI) microscope employing a LaB_6 filament with an acceleration voltage of 200 kV. The samples for TEM studies were dispersed in ethanol and dripped onto a carbon-coated copper grid.

UV/Vis Spectroscopy: After the proper equilibrium time (24 h, 120 h and 168 h), aliquots of each flask were collected and diluted by different factors. The samples were then measured in a Shimadzu UV-2550 UV/Vis spectrophotometer.

Isothermal Titration Calorimetry (ITC): Measurements of the enthalpy changes in the adsorption process of PhCs onto MWCNT were performed in triplicate using a CSC-

4200 microcalorimeter (Calorimeter Science Corp.) controlled by ItcRun software with a 1.75 mL reaction cell (sample and reference). The entire calorimetry procedure was calibrated chemically and electrically to the heat of protonation for tris(hydroxymethyl) aminomethane and the joule effect, respectively [20]. The titrations were carried out via step-by-step injections (10 μL) of concentrated PhC titrant solutions using an instrument-controlled gas-tight Hamilton syringe (250 μL) at 60 min intervals between each injection. Aliquots of concentrated PhC solutions, dissolved in water, were added to a sample cell containing a suspension of 1 mg of MWCNT in aqueous solution. The solution was titrated in the sample cell stirred at 300 rpm by a helix stirrer, and measurements were carried out at a constant temperature of 25.000 ± 0.001 °C. Distilled water was used for preparing all solutions and carbon nanotube suspensions. The concentrations of the initial PhC solutions were chosen so that after each injection, the resulting concentrations in the sample cell would become identical to the concentrations used to obtain the adsorption isotherms.

3. Results and discussion

3.1. Carbon nanotube characterization

From the thermogravimetric analysis (figure 1a) and SEM and TEM images (examples can be found in figure 1b and figure 1c, respectively), the multi-walled carbon nanotube sample has a purity higher than 90%, with tube diameter of approximately 10–40 nm (with a predominance of tubes having an average diameter of approximately 13 nm). Its surface area, determined by nitrogen adsorption/desorption isotherms at 77 K using the BET equation, is on the order of 188 m^2 g^{-1}. These data are in agreement with the information provided by the supplier of the material, as previously presented.

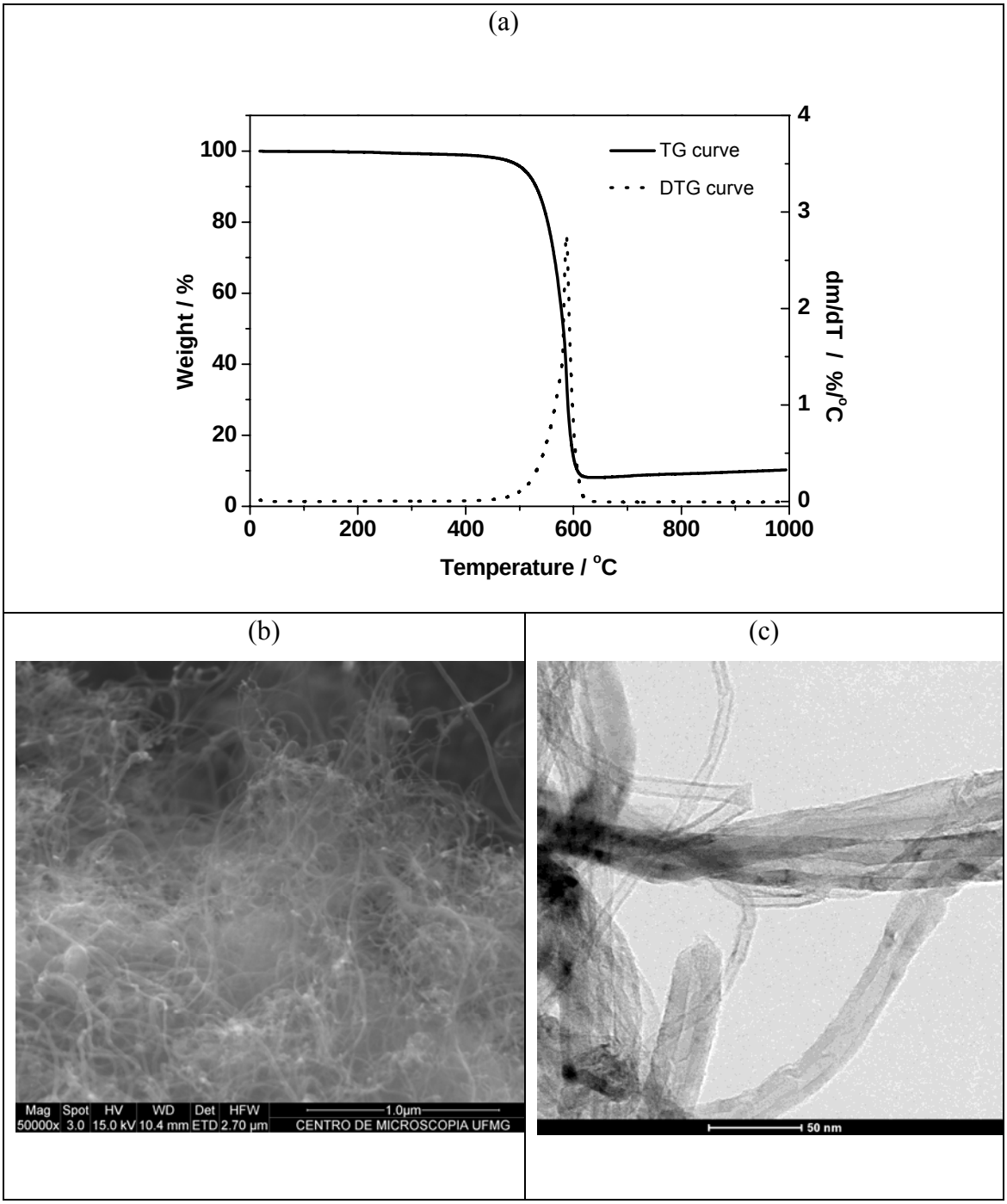

Figure 1. (a) TGA and DTG curves, (b) scanning electron micrograph and (c) transmission electron images of MWCNT samples.

3.2. Adsorption isotherms

Generally, when activated carbon (the most common adsorbent) is employed in adsorption experiments, a long time is required to reach thermodynamic equilibrium [6,13]. Considering this information and the fact that the use of CNTs for adsorption of contaminants is a developing field, the influence of the equilibrium time (24 h, 120 h

and 168 h) on the adsorption process was evaluated. We observed that the adsorption of the different phenolic compounds onto the MWCNTs reaches thermodynamic equilibrium in 24 h or less. No significant change was observed after 24 h (at 120 h or 168 h) in all cases. In fact, Peng and co-workers [13] observed that the process of the adsorption of 1,2-dichlorobenzene on as-grown and graphitized CNTs requires 40 min to reach equilibrium. Liao et al., [12] evaluating the adsorption time of resorcinol on pristine and HNO_3-treated MWCNTs, observed that after only 1 min of shaking, the amount of adsorbed molecules reaches 60% of the total amount adsorbed at equilibrium. It was suggested that this short time could be related to the fact that CNTs do not have the same porous structure as activated carbon in which the adsorbent molecules must move from the exterior surface to the inner surface of the pores to achieve equilibrium [13].

The adsorption isotherms of the phenolic compounds on MWCNT are shown in figure 2 in which the amount of each adsorbed PhC (mg g^{-1}) of MWCNT is plotted against the equilibrium concentration of the respective PhC (mg mL^{-1}). The curves were obtained after 24 h to achieve thermodynamic equilibrium.

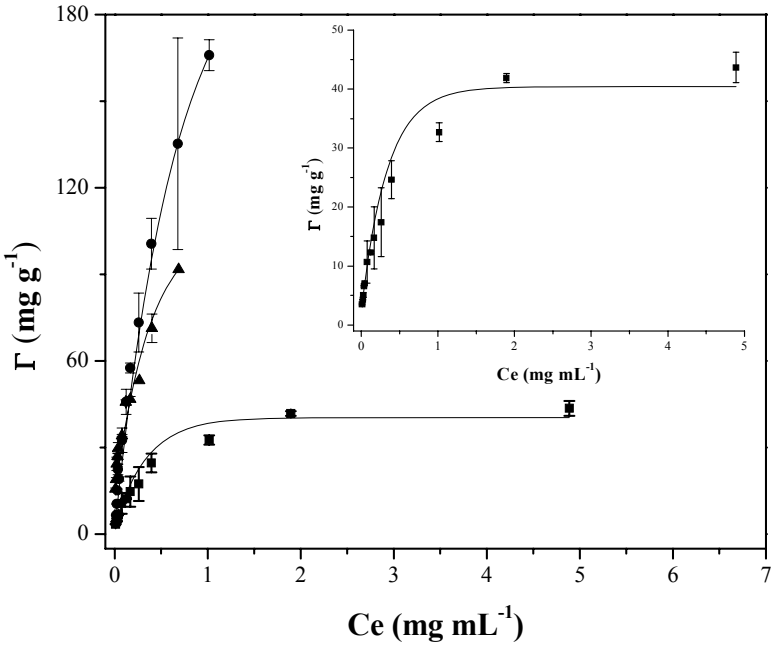

Figure 2. Adsorption isotherms of phenol (■), 2-methylphenol (▲) and 4-chlorophenol (●) on MWCNT. The isotherm of phenol is also presented in detail in the inset.

The isotherms are non-linear and of the same type. They are characterized by an increase in the amount of PhC adsorbed with increasing equilibrium concentrations,

followed by a tendency toward the formation of a plateau at higher concentrations, which represents the maximum adsorption capacity. All curves present a shape suggesting a process that can be described by the Langmuir model as clearly observed in the phenol curve that is reproduced in the inset of figure 2. This inset curve shows a maximum adsorption of approximately 43 $mg \cdot g^{-1}$. The presence of chlorine and methyl groups enhances the adsorption onto the MWCNTs. The isotherms clearly indicate maximum adsorption following the order phenol < 4-chlorophenol < 2-methylphenol. The amount of adsorbed 2-methylphenol (in mg) per gram of MWCNT reaches values as high as 166 $mg \cdot g^{-1}$ at an equilibrium concentration of 1.0 mg mL^{-1} (see figure 2). This amount is considerable and makes possible the use of MWCNTs as an adsorbent for this group of wastewater contaminants.

The equations of Langmuir and Freundlich are the most commonly applied models for representing the nonlinear adsorption of organic chemicals, such as phenolic compounds, to activated carbon, charcoal, and carbon nanotubes [14,15]. Both models were employed to fit the experimental data presented in figure 2.

The Langmuir isotherm can be derived by assuming an ideal system in which the adsorbent molecules adsorb onto the adsorbate surface at well-defined sites forming a homogeneous monolayer. Each site can adsorb only one molecule, and the energy involved in the adsorption of one adsorbent molecule is the same for all sites on the adsorbate surface and is independent of the presence or absence of other molecules on the adjacent sites. There is no interaction between adjacent adsorbent molecules. Equation 2 represents the mathematical expression of the Langmuir model:

$$\Gamma = \frac{\Gamma_{\max} K_L C_e}{1 + K_L C_e} \tag{2}$$

in which C_e is the equilibrium PhC concentration (mg mL^{-1}), Γ is the amount of PhC adsorbed (mg g^{-1}), K_L is a Langmuir constant related to the affinity of the binding sites (adsorption energy), and Γ_{max} (mg g^{-1}) is a Langmuir constant related to the maximum monolayer adsorption capacity, which describes a saturated monolayer of solute molecules on the adsorbent surface (the theoretical saturation capacity of the monolayer) and specifies that further adsorption will contribute to a prohibitive increase in the Gibbs free energy of the interface.

The Freundlich empirical isotherm assumes the existence of heterogeneous surfaces having different sites with diverse energies of adsorption and the possibility for the

formation of multilayers:

$$\Gamma = K_F C_e^{1/n} \tag{3}$$

in which C_e and Γ were previously described. K_F ($mg^{(1-1/n)}$ $mL^{(1/n)}$ g^{-1}) is the Freundlich constant describing the adsorption capacity and the energy distribution of the adsorption sites. The Freundlich constant, *n,* describes the magnitude of the adsorption driving force.

The Langmuir and Freundlich equations can be fitted to the data by linear regressions using their linearized forms as follows:

$$\frac{C_e}{\Gamma} = \frac{1}{\Gamma_{max}} C_e + \frac{1}{K_L \Gamma_{max}} \tag{4}$$

$$\ln \Gamma = \ln K_F + \frac{1}{n} \ln C_e \tag{5}$$

in which plots of $\frac{C_e}{\Gamma}$ versus C_e and lnΓ versus lnC_e allow for the calculation of the Langmuir and Freundlich constants, respectively. The values obtained following these data fittings are presented in tables 1 and 2.

Table 1. Langmuir constants obtained by the linear forms of the equations.

PhC	LANGMUIR			
	Γ_{max} / mg g^{-1}	K_L / g mg^{-1}	Linear Equation	R^2
phenol	46.08	3.34	Ce/Γ = 0,02174Ce + 0,00652	0.989
4-chlorophenol	95.97	9.22	Ce/Γ = 0,01042Ce + 0,00113	0.9280
2-methylphenol	242.72	1.93	Ce/Γ = 0,00412Ce + 0,00214	0.951

Table 2. Freundlich constants obtained by the linear forms of the equations.

PhC	FREUNDLICH			
	K_F $mg^{(1-1/n)}$ $mL^{(1/n)}$ g^{-1}	1/n	Linear Equation	R^2
phenol	29.76	0.45	lnΓ = 0,4531lnCe + 3,3931	0.968
4-chlorophenol	100.41	0.40	lnΓ = 0,39622lnCe + 4,60925	0.984
2-methylphenol	194.75	0.75	lnΓ = 0,74531lnCe + 5,27177	0.973

Taking into account the quality of the fit given by the correlation coefficient (R^2) in table 1, both adsorption models adjust the data in a reasonable way. The constants Γ_{max} and K_F indicate the same tendency observed in the isotherms: 2-methylphenol exhibits greater adsorption than 4-chlorophenol, which exhibits greater adsorption than phenol. However, the Langmuir Γ_{max} values seem to be a more reasonable fit in relation to the data (see figure 2). Therefore, apart from the mathematical quality of the fit, considering the Γ_{max} values the Langmuir model appears to be more applicable. For example, Γ_{max} observed in the isotherm is approximately 43 mg g^{-1}, and Γ_{max} obtained from the fit was 46.08 mg g^{-1} (table 1) for phenol.

In the Freundlich approach, the magnitude of 1/n quantifies the "favorability" of adsorption and the degree of heterogeneity of the CNT surface. If 1/n is less than unity, suggesting a favorable adsorption with a negative $\Delta_{ads}G^o$, the adsorption capacity increases, and new adsorption sites form [11,21]. Considering the data presented in table 1, the values of 1/n are less than unity for phenol, 2-methylphenol and 4-chlorophenol, reinforcing the assertion that the adsorption of PhCs on MWCNTs is favorable.

3.3. Microcalorimetry Experiments

The energy released or absorbed as heat in a thermodynamic process can be measured by equipment and calorimetric techniques that allow its detection. Among these, isothermal titration microcalorimetry has been widely used for the determination of many molecular processes due to its high sensitivity and its ability to detect energy flows occurring in a given process on the order of 10^{-9} J.

Curves of the adsorption enthalpy change ($\Delta_{ads}H$) versus the equilibrium concentrations of phenol, 2-methylphenol and 4-chlorophenol on MWCNT, obtained from ITC measurements at 298 K, are shown in figure 3.

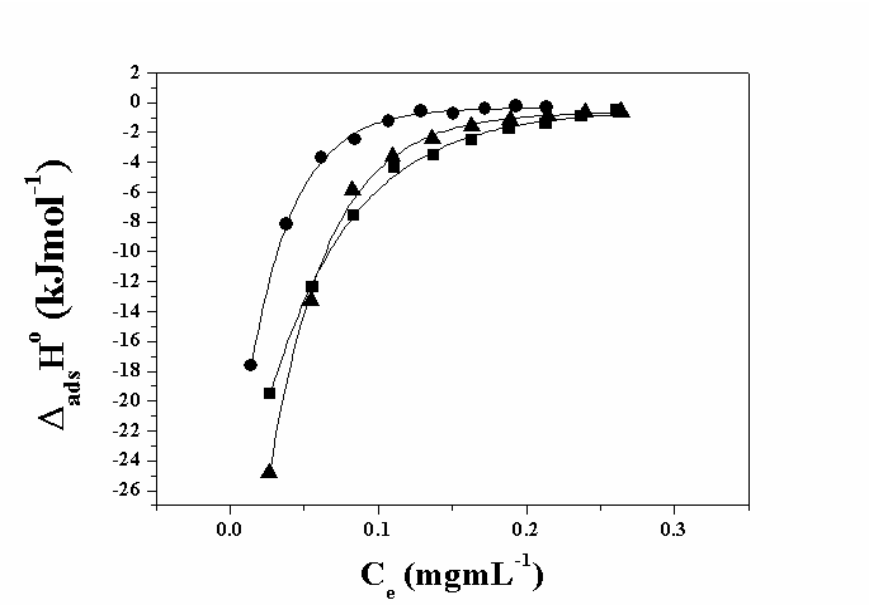

Figure 3. ΔH of adsorption (kJ mol^{-1}) versus equilibrium concentration (mg mL^{-1}) for the adsorption process of phenol (■), 2-methylphenol (▲) and 4-chlorophenol (●) on MWCNT.

The total value of $\Delta_{ads}H$ attributed to adsorption process may be expressed as follows:

$$\Delta_{ads}H = \Delta_{deh}H_{ChP-H_2O} + \Delta_{des}H_{MWCNT-H_2O} + \Delta_{\text{int}}H_{H_2O-H_2O} + \Delta_{\text{int}}H_{ChP-ChP(MWCNT)} + \Delta_{\text{int}}H_{MWCNT-ChP} \quad (6)$$

According to equation 6, the $\Delta_{ads}H$ values reflect the contributions of five processes: the $\Delta_{deh}H_{PhC-H_2O}$ and the $\Delta_{deh}H_{MWCNT-H_2O}$, which are the enthalpy changes of dehydration for the specific phenolic compound and MWCNT, respectively (both endothermic); the exothermic $\Delta_{\text{int}}H_{H_2O-H_2O}$ that is related to the interaction between water molecules released during the desolvation process; $\Delta_{\text{int}}H_{PhC-PhC(MWCNT)}$ (exothermic or endothermic), which describes the interaction energy between molecules of the phenolic compound adsorbed onto adjacent sites on the MWCNT surface; and the exothermic $\Delta_{\text{int}}H_{MWCNT-PhC}$ that indicates the intensity of the enthalpic interaction between the PhC molecules and the carbon nanotube surface. As is well known, the $\Delta_{deh}H_{PhC-H_2O}$, $\Delta_{\text{int}}H_{ChP-ChP(MWCNT)}$ and $\Delta_{\text{int}}H_{MWCNT-PhC}$ values differ from one phenolic compound to another.

As observed in figure 3, the $\Delta_{ads}H$ is negative, which means that the adsorption process onto MWCNT is exothermic for all phenolic compounds and approaches zero for equilibrium concentrations of the order of 0.1-0.2 mg mL^{-1}. At the beginning of the adsorption process, the amount of energy released as heat ($\Delta_{ads}H$) in the adsorption of 2-methylphenol is greater than that liberated in the adsorption of phenol, which, in turn, is greater than the energy released in the adsorption of 4-chlorophenol. With increasing PhC concentration, the $\Delta_{ads}H$ values become less negative showing remarkable evidence for the existence of different sites at the MWCNT interface that accomplish specific interactions with the distinct phenolic compounds. These interactions are dependent on the electron density of the ring, which is modulated by its functional groups (CH_3, H and Cl). The interactions caused by dispersion forces (lower energy) occur only after saturation of these specific sites.

As previously indicated, although the adsorption isotherms have adjustable profiles within the Langmuir equation, microcalorimetry measurements show that CNT surfaces are not homogeneous regions. If an adsorption process follows the Langmuir model, constant values of $\Delta_{ads}H$ would be expected throughout the process. This finding suggests that models like those of Freundlich and others, which describe the adsorption on heterogeneous surfaces that have sites at which the adsorption occurs with different energies, seem to be more realistic for the systems studied in this work. In fact, considering the adjustments of the adsorption isotherms, the quality of the mathematical fit should not be a defining parameter to choose between models with such different physicochemical implications.

According to several researchers [19,22-24], there are seven possible adsorption sites on a bundle of carbon nanotubes: (i) inner (internal) nanotube cavity, (ii) inter-wall spaces (in the case of MWCNTs), (iii) interstitial channels between neighboring nanotubes in the bundle, (iv) external grooves on the periphery of a nanotube bundle, (v) external surface, (v) partial coating of the external surface by nanometer-thick layered carbon, and (vii) carbon-coated catalyst particles. The last two sites are present in the case of unpurified samples. Yang and Xing presented evidence that most spaces available for adsorption of N_2 molecules onto MWCNTs are on the cylindrical external surface. N_2 did not readily adsorb onto the inner cavities because of blocking impurities (i.e., amorphous carbons), nor did it adsorb in the inter-wall spacing because of the small interlayer spacing (0.335 nm) [19]. According to Sheng and co-workers [16], ionizable aromatic compounds were thought to preferentially occupy the external graphene surface of MWCNTs during the initial adsorption process, while the overall

adsorption included contributions from both adsorptions on the graphene surface and pore filling. Liao and coworkers indicated that the adsorption of resorcinol onto MWCNT is not dependent on the porous structure, but that the chemical properties of the surface, rather than specific surface areas or pore volumes, are crucial factors do determine the final adsorption ability of MWCNTs [12]. This evidence validates the rapid adsorption of organic contaminants on CNTs discussed previously. Therefore, based on the data in figure 3 and on the assumption that the external surface is the primary, or at least the preferential, adsorption site, we can indicate the existence of different functional groups chemisorbed onto the surface of the MWCNTs employed in the present work (i.e., carbonyl, carboxylic, hydroxyl). In fact, Sheng and coworkers show the presence of functional groups such as carboxylic, lactone and phenolic groups on pristine CNT surfaces synthesized by CVD [16]. As previously described, functional groups chemisorbed onto the surfaces of carbon materials have a remarkable influence on the adsorption process, even in small quantities [10].

Several studies indicate the π-π dispersion interactions as those primarily responsible for the adsorption of aromatic compounds on CNTs, by the closeness of respective aromatic rings [3,6,15,25]. According to Sheng et al., hydrogen bonding, hydrophobic interactions, electrostatic interactions and Lewis acid-base interactions could also be present [16]. Electrostatic and Lewis acid-base interactions are not present in our case because at the solution pH used for the experiments, the PhCs are undissociated (uncharged). This result was also observed by Dias-Florez and colleagues studying the adsorption of phenol on N-doped carbon nanotubes [9]. As previously indicated by the values of $\Delta_{ads}H$ (figure 3), dispersion forces are not the only forces responsible for the adsorption process of PhCs onto MWCNTs. We can speculate that hydrogen bonding could be responsible for the large negative values of $\Delta_{ads}H$ observed for all phenolic compounds. In fact, the $\Delta_{ads}H$ values are on the order of those reported for hydrogen bonding interactions (10–40 kJ mol^{-1}). The inductive effect, caused by the functional groups (CH_3, H and Cl) present in 2-methylphenol, phenol and 4-chlorophenol, respectively, interacts with the oxygen functional groups on the MWCNT surface through phenolic OH and resonance effects can be the reason for the difference in the enthalpic energies observed in figure 3. In other words, $\Delta_{ads}H$ in the adsorption of 2-methylphenol has a larger negative value than that of phenol, which in turn has a larger negative value than that of 4-chlorophenol. The CH_3 groups are electron donating (Hammett σ is negative), and the Cl groups are electron withdrawing (Hammett σ is positive). Yang and colleagues [17], analyzing the relationship between solvatochromic

and Dubinin-Astakhov model parameters, concluded that hydrogen-bonding interactions play an important role in the adsorption of anilines and phenols by carbon nanotubes in which the solutes may act as hydrogen-bond donors, and the carbon nanotubes act as hydrogen-bond acceptors. Franz and colleagues verified that the adsorption mechanisms of different aromatic compounds (including phenol) onto activated carbon are influenced by the properties of the oxygen-containing functional groups on the aromatic adsorbate, especially their ability to hydrogen bond and their activating/deactivating influence on the aromatic ring [10].

The evaluation of the presence of different functional groups chemisorbed onto the CNT external walls is not a simple experimental task. Generally, combinations of different techniques, such as infrared, Raman and XPS spectroscopies, are employed. To our knowledge, this study is the first to use microcalorimetry to detect the existence of distinct functional groups on the external walls of carbon nanotubes.

3.4. Thermodynamic properties

The change in the standard Gibbs free energy for the adsorption process ($\Delta_{ads}G^o$) is calculated from the thermodynamic relationship as follows:

$$\Delta_{ads} G^o = -RT \ln K^o \tag{7}$$

in which K^o is the equilibrium constant for the adsorption process, R is the universal gas constant, and T is the temperature in Kelvin.

The equilibrium constant for the adsorption process, K^o, can be obtained if $\mu_i^{\text{int}} = \mu_i^{sol}$, and $\mu_i^{sol,or,\text{int}} = \mu_i^o + RT \ln a_i^{sol,or,\text{int}}$ in which μ_i^{int} is the chemical potential of *i* (in our case PhC) adsorbed at the MWCNT–solution interface; μ_i^{sol} is the chemical potential of *i* in solution (at equilibrium); μ_i^o is the chemical potential of *i* at a standard condition; and $a_i^{sol,or,\text{int}}$ is the activity of *i* (in solution or at the MWCNT–solution interface). After some manipulation of the equations, we obtain the following relationship:

$$\ln K^o = \ln\left(\frac{a_i^{\text{int}}}{a_i^{sol}}\right) = \ln\left(\frac{\gamma_i^{\text{int}}}{\gamma_i^{sol}} \cdot \frac{C_i^{\text{int}}}{C_i^{sol}}\right) \tag{8}$$

in which C_i^{int} is the concentration of the adsorbed PhC at the MWCNT–solution interface (mg g^{-1}), C_i^{sol} is the concentration of the PhC in solution at equilibrium (mg mL^{-1}), γ_i^{int} is the activity coefficient of the adsorbed PhC, and γ_i^{sol} is the activity coefficient of the PhC in solution at equilibrium conditions.

As the concentration of the solute in the solution approaches zero, the activity coefficient approaches unity, and Eq. (8) reduces to the following form:

$$\ln K^o = \ln\left(\frac{a_i^{\text{int}}}{a_i^{sol}}\right) = \ln\left(\frac{C_i^{\text{int}}}{C_i^{sol}}\right), \text{ with } \frac{C_i^{\text{int}}}{C_i^{sol}} = \frac{\Gamma}{C_e} \tag{9}$$

The values of $\ln K^o$ can be obtained by plotting $\ln(\Gamma/C_e)$ versus C_e and by extrapolating C_e to zero. The straight line obtained is fitted to the points based on a least-squares analysis. Its intercept with the vertical axis yields the values of $\ln K^o$ that are used in Eq. (7).

The change in the standard entropy of the adsorption process ($\Delta_{ads}S^o$) is calculated using the classic thermodynamic equation (T = 298 K):

$$\Delta_{ads} G^o = \Delta_{ads} H^o - T\Delta_{ads} S^o \tag{10}$$

The values of $\Delta_{ads}H^o$ for each PhC were obtained from the data presented in figure 3 following the extrapolation of C_e to zero using an exponential fit (the solid lines in figure 3).

The values obtained for the thermodynamic properties are listed in table 3. The adsorption of PhC onto MWCNT is a spontaneous process ($\Delta_{ads}G^o < 0$). The $\Delta_{ads}G^o$ values follow the order: phenol < 2-methylphenol < 4-chlorophenol.

Table 3. Thermodynamic properties obtained for the adsorption of phenolic compounds

on MWCNTs.

PhC	Thermodynamic properties				
	$\Delta_{ads}G^o$ / kJ mol^{-1}		$\Delta_{ads}H^o$ / kJ mol^{-1}	$T\Delta_{ads}S^o$ / kJ mol^{-1}	
	Langmuir	Thermodynamic		Langmuir	Thermodynamic
phenol	-12.48	−13.18	−31.08	-18.60	−17.90
2-methylphenol	-15.22	−15.07	−47.57	-32.34	−32.50
4-chlorophenol	-16.81	−18.01	−28.12	-11.31	−10.11

The value of $\Delta_{ads}S^o$ is negative, indicating an entropy decrease in the PhC molecules adsorbed onto the MWCNT–solution interface, caused primarily by a decrease in the configuration entropy of the PhC molecules. As the value of $\Delta_{ads}S^o$ is negative, the decrease in the Gibbs free energy of the system is caused by the negative $\Delta_{ads}H^o$, so the adsorption process is enthalpically driven. The specific interactions of the PhC molecules with the functional groups chemisorbed onto the surface of the MWCNTs (probably hydrogen bonds) are the driving force for the adsorption process. As observed in figure 3 and table 3 the enthalpy of interaction is higher in the adsorption of the 2-methylphenol ($\Delta_{ads}H^o$ is more negative). Thus, the decrease in the configurational and conformational entropies is higher for this compound during its adsorption onto the MWCNT-interface (the $\Delta_{ads}S^o$ values are more negative than those of the other PhCs).

Shen and colleagues [15] and Chen and colleagues [8] obtained the same behavior (enthalpic driven adsorption process) for the adsorption of nitroaromatic compounds (including 4-nitrophenol) and atrazine, respectively, on as-grown and oxidized MWCNTs.

4. Conclusions

This report describes, for the first time, the use of microcalorimetric techniques to evaluate the surface of an MWCNT sample and its interactions with phenolic compounds. The adsorption thermodynamics of phenol, 2-methylphenol and 4-chlorophenol on pristine multi-walled carbon nanotubes (MWCNTs) were evaluated using isothermal titration calorimetry (ITC) as the primary technique. The adsorption of any phenolic compound onto MWCNTs is a spontaneous process ($\Delta_{ads}G^o < 0$). Small variations in the chemical structures of phenolic compounds can considerably alter their

energies of adsorption. The decrease in the Gibbs free energy of adsorption follows the order phenol < 2-methylphenol < 4-chlorophenol. The adsorption process is enthalpically driven, and the ITC data shows that the MWCNT interfaces have sites that allow specific interactions with phenolic compounds, not only hydrophobic and π-π dispersion interactions. Therefore, we can speculate that hydrogen bonding could be responsible for the large negative $\Delta_{ads}H^{o}$ values observed for all phenolic compounds.

The isotherms obtained at 298 K were fitted by the Langmuir and Freundlich models. Taking into account the quality of the fit given by the correlation coefficient (R^2), both adsorption models adjust the data in a reasonable way. However, according to the $\Delta_{ads}H^{o}$ values, models like that of Freundlich and others, which describe the adsorption on heterogeneous surfaces that have sites where adsorption occurs with different energies, seem to be more realistic models for the systems studied in this work.

References

[1] Kahru A and Dubourguier H-C 2010 *Toxicology* **269** 105-19

[2] Iijima S 1991 *Nature* **354** 56–8

[3] Lin D and Xing B 2008 *Environ. Sci. Technol.* **42** 7254-9

[4] Trigueiro J P C, Borges R S, Lavall R L , Calado H D R and Silva G G 2009 *Nano Res.* **2** 733-9

[5] Long R Q and Yang R T 2001 *J. Am. Chem. Soc.* **123** 2058–9

[6] Liao Q, Sun J and Gao L 2008 *Carbon* **46** 553-5

[7] Castillejos-López E, Nevskaia D M, Munoz V and Guerrero-Ruiz A 2008 *Carbon* **46** 870-5

[8] Chen G-C, Shan X-Q, Zhou Y-Q, Shen X, Huang H-L and Khan S U 2009 *J. Hazard. Mater.* **169** 912-8

[9] Diaz-Florez P E, López-Urías F, Terrones M and Rangel-Mendez J R 2009 *J. Colloid Interf. Sci.* **334** 124-31

[10] Franz M, Arafat H A and Pinto N G 2000 *Carbon* **38** 1807-19

[11] Kuo C-Y 2009 *Desalination* **249** 976-82

[12] Liao Q, Sun J and Gao L 2008 *Colloid. Surface.* A **312** 160-5

[13] Peng X, Li Y, Luan Z, Di Z, Wang H, Tian B and Jia Z 2003 *Chem. Phys. Lett.* **376** 154-8

[14] Salam M S and Burk R C 2008 *Appl. Surf. Sci.* **255** 1975-81

[15] Shen X-E, Shan X-Q, Dong D-M, Hua X-Y and Owens G 2009 *J. Colloid. Interf. Sci.***330** 1–8

[16] Sheng G D, Shao D D, Ren X M, Wang X Q, Li J X, Chen Y X and Wang X K 2010 *J. Hazard. Mater.* **178** 505-16

[17] Yang K, Wu W, Jing Q and Zhu Z 2008 *Environ. Sci. Technol.* **42** 7931–6

[18] Ania C O and Bandosz T J, Surface chemistry of activated carbons and its characterization, In: Bandosz T J (Ed.), 2006 *Activated Carbon Surfaces in Environmental Remediation* (Oxford: Elsevier), pp 159-230

[19] Yang K and Xing B 2007 *Environ. Pollut.* **145** 529–37

[20] Barbosa A M, Santos I J B, Ferreira G M D, da Silva M D H, Teixeira A V N D and da Silva L H M 2010 *J. Phys. Chem.* B **114** 11967-74

[21] Ozcan A S, Erdem B and Ozcan A 2004 *J. Colloid. Interf. Sci.* **280** 44–54

[22] Zhao J, Buldum A, Han J and Lu J P 2002 *Nanotechnology* **13** 195-200

[23] Agnihotri S, Rostam-Abadi M and Rood M J 2004 *Carbon* **42** 2699-2710

[24] Agnihotri S, Mota J P B, Rostam-Abadi M and Rood M J 2006 *Carbon* **44** 2376-83

[25] Zhang Y, Yuan S L, Zhou W W, Xu J J and Li Y J 2007 *J. Nanosci. Nanotechno.* **7** 2366–75

Surface heterogeneity effect on azodyes adsorption onto multiwalled carbon nanotubes

Abstract

The adsorption thermodynamics of the azo dyes acid yellow 42 (AY), acid black 210 (AB) and acid green 68:1 (AG) onto pristine multi-walled carbon nanotubes (MWCNTs) was evaluated by determining the following thermodynamic adsorption parameters: adsorption standard free energy ($\Delta_{ads}G^{o}$), adsorption standard enthalpy ($\Delta_{ads}H°$) and adsorption standard entropy ($\Delta_{ads}S°$). The adsorption of all azo dyes onto MWCNTs was a thermodynamically spontaneous process and the decrease in $\Delta_{ads}G^{o}$ values follows the order AG < AB < AY. The increase of oxidized sites on MWCNT surface enabled a decrease of adsorption capacity of AY, compared with raw MWCNT. The adsorption of all azodyes is directly proportional with the ionic strength of solution. Isothermal Titration Calorimetry (ITC) data show that the adsorption process is enthalpically driven for all azodyes with contribution of entropy change in the spontaneity of AY adsorption onto MWCNT. The surface of the MWCNT has sites with different energetic potentials that allow electrostatic interactions with azo dye compounds, not only π–π dispersion interactions. The ITC technique provides a more reliable interpretation of the surface chemistry of MWCNT and of the interactions in an adsorption process in comparison with the van't Hoff approximation.

1. Introduction

Wastewater from dyeing industries, such as textiles, dyestuff, paper and leather, is a hazardous discharge because of its toxicity and environmental pollution. Dyes added to natural waters are also aesthetically objectionable for drinking and other purposes [1]. Their synthetic origins and complex aromatic molecular structure implies in low biodegradability.

Several methods are employed for dyes removal from industrial effluents, and adsorption is regarded as an efficient process because of its low initial cost, ease of operation and design flexibility and simplicity [2].

Among adsorbents applied for dyes removal [3-10], carbon nanotubes (CNTs) are becoming attractive because of the following characteristics: capacity to adsorb colored compounds from aqueous solutions [11-13] and large surface area and high porosity [14]. However, to our best knowledge there are only four papers published, reporting the adsorption thermodynamics of azo dyes on CNTs [1,13,15-16], none of which measuring directly the adsorption standard enthalpy by means of isothermal titration calorimetry (ITC). Machado *et al*. [1] found that the adsorption of the azo dye Reactive Red M-2BE onto multi-walled carbon nanotubes presented a maximum adsorption capacity of 312.3 mg g^{-1} at 298 K. Although the process was endothermic ($\Delta_{ads}H^{o}$ = 33.13 kJ mol^{-1}), the positive variation in the standard entropy of adsorption ($\Delta_{ads}S°$ = 208.0 J K^{-1} mol^{-1}) guarantees the spontaneity of the adsorption phenomenon. The authors also suggested a mechanism of adsorption with three steps: the functional groups of the MWCNTs are protonated; agglomerates of dyes are dispersed in the aqueous solution; and the negatively charged dyes are electrostatically attracted to the positively charged surface of the MWCNTs. Several works found in literature describe the thermodynamics of dye adsorption onto MWCNT, with all of them applying Van't Hoff approximation to determine $\Delta_{ads}H°$. Kuo *et al*. [13] found lower values of maximum adsorption capacity of Direct Yellow 86 (54.9 mg g^{-1}) and Direct Red 224 (52.1 mg g^{-1}) at 35 °C onto CNT. The process was endothermic ($\Delta_{ads}H°$ = 13.69 kJ mol^{-1} for DY 86; $\Delta_{ads}H°$ = 24.29 kJ mol^{-1} for DR 224), and $\Delta_{ads}S°$ was positive (139.51 and 177.83 J K^{-1} mol^{-1} for AY 86 and AR 224, respectively). The authors suggest that the adsorption of both dyes onto CNT was driven by a physisorption process. The same conclusion was taken by Wu [15], who studied the adsorption of Procion Red MX-5B onto CNT and found that the maximum amount dye adsorbed (Γ_{max}) ranges from 29.94 to 44.64 mg g^{-1} between pH 6.5-10 and temperatures between 281 and 321 K. The thermodynamic properties revealed a spontaneous ($\Delta_{ads}G°$ = –29.79 kJ mol^{-1} at 281 K, pH = 6.5), endothermic process (31.55 kJ mol^{-1} at pH 6.5), with $\Delta_{ads}S°$ = 216.99 J mol^{-1} K^{-1}. Therefore, information about the influence of MWCNT surface on the adsorption mechanism is required.

This study aims to investigate the adsorption of three azo dyes (AD) on multiwalled carbon nanotubes (MWCNT) from aqueous solutions and also describes, for the first time, the nature of CNTs surface and the interactions between CNTs and adsorbates by means of isothermal titration calorimetry.

2. Material and Methods

2.1. Adsorbates

The adsorbates, AY [chemical formula: $C_{32}H_{24}N_8Na_2O_8S_2$, MW: 758.69 g mol^{-1}, λ_{max} = 411 nm], AB [chemical formula: $C_{34}H_{25}K_2N_{11}O_{11}S_3$, MW: 938.02 g mol^{-1}, λ_{max} = 462 nm] and AG [chemical formula: $C_{34}H_{25}N_9O_{13}S_3$, MW: 863.8098 g mol^{-1}, λ_{max} = 603 nm] were donated by BASF Corp., Brazil. The structures of AY, AB and AG dyes are illustrated in Figure 1. An exact weighted quantity of each dye was dissolved in distilled water to prepare stock solutions (1 mg mL^{-1}). All solutions employed in the experiments were obtained by successive dilutions with distilled water.

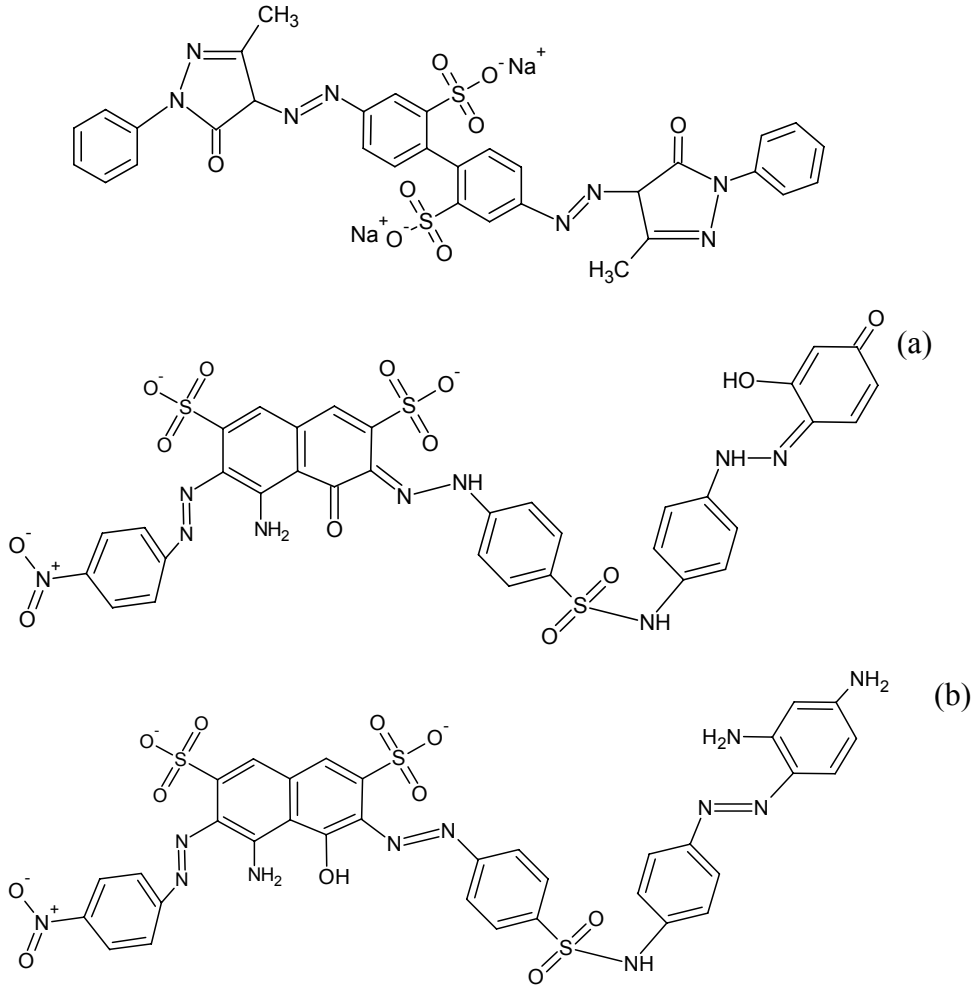

Figure 1. Molecular structures of (a) AY, (b) AG and (c) AB.

2.2. Characterization of CNT

Multi-walled carbon nanotubes C_{TUBE} 100 were purchased from CNT CO., LTD., Korea. The following technical specification of the MWCNT was supplied by the manufacturer: average diameter: 10-40 nm; length: 1-25 μm; purity: 93 wt% min.; contaminants: 7 wt% max.; bulk density: 0.03-0.06 g cm^{-3}; specific surface area: 150-250 m^2 g^{-1}.

N_2 adsorption: The specific surface area and porosity were determined at 77 K with a Nova 1000 volumetric adsorption analyzer, acquired from Quantachrome Corp., USA. Brunauer-Emmett-Teller (BET) and Barret, Joyner and Halenda (BJH) methods were used to determine BET surface area and pore size distribution, respectively.

Thermogravimetric Analysis (TG): Thermogravimetric measurements were performed in a TA Instruments SDT 2960 simultaneous TG/DTA at 5°C min^{-1} in dry air flow of 100 mL min^{-1} between 25 and 1000 °C in alumina crucibles. The degradation temperature was determined by T_{onset}. Scanning electron microscopy (SEM) and transmission electron microscopy (TEM) were performed with a JEOL JSM-8404 scanning microscope and a JEOL JEM-2010 transmission microscope, respectively.

Transmission Electron Microscopy: Transmission electron microscopy (TEM) was carried out with a Tecnai G-20 (FEI) microscope employing a LaB_6 filament with an acceleration voltage of 200 kV. The samples for TEM studies were dispersed in ethanol and dripped onto a carbon-coated copper grid.

UV/Vis Spectroscopy: After the proper equilibrium time (24 h), aliquots of each flask were collected and diluted by different factors. The samples were then measured in a Thermo Scientific Evolution 300 UV/Vis spectrophotometer.

Isothermal Titration Calorimetry (ITC): Measurements of the enthalpy changes in the adsorption process of azo dyes onto MWCNT were performed in triplicate using a CSC-4200 microcalorimeter (Calorimeter Science Corp.) controlled by the ItcRun software with a 1.75 mL reaction cell (sample and reference). The entire calorimetry procedure was calibrated chemically and electrically to the heat of protonation for tris(hydroxymethyl) aminomethane and the Joule effect, respectively [20]. The titrations were carried out via step-by-step injections (10 μL) of concentrated azo dyes titrating solutions using an instrument-controlled gas-tight Hamilton syringe (250 μL) at 60-min intervals between each injection. Aliquots of concentrated azo dyes solutions, dissolved in water, were added to a sample cell containing a suspension of 1.35 mg of MWCNT in aqueous solution. The solution was titrated in the sample cell stirred at 300 rpm by a helix stirrer, and measurements were carried out at a constant temperature of 25.000 ± 0.001 °C. Distilled water was used for preparing all solutions and carbon nanotube

suspensions. The concentrations of the initial dyes solutions were chosen so that after each injection, the resulting concentrations in the sample cell would become identical to the concentrations used to obtain the adsorption isotherms.

2.3. Surface modification of CNT

MWCNT surface was modified to study the effect of oxidation on the adsorption of dye. Surface modification procedures were employed as described elsewhere [17,18].

MWCNT acidification. 100 mL of concentrated HNO_3 were added to 1 g of MWCNT at constant magnetic stirring for 24 h at room temperature. This procedure yielded acidified carbon nanotubes labeled as MWCNT-acid.

MWCNT oxidation. 100 mL of H_2O_2 at 18 % (v/v) were added to 1 g of MWCNT at constant magnetic stirring for 4 h at 80 °C. Carbon nanotubes obtained by this method were labeled as MWCNT-oxid.

Modified MWCNT were filtered, washed thoroughly with distilled water and dried at (378 ± 5) K for 12 h, prior to use.

2.4. Adsorption experiments

Adsorption experiments were carried out in duplicate with a set of 40-mL glass centrifuge tubes sealed with headspace screw caps, where solutions of dye (20 mL) with different initial concentrations (C_0) (0.01 – 0.50 mg mL^{-1}) were mixed with 15 mg of MWCNT. The tubes were shaken manually for 10 minutes and placed in a thermostatically controlled bath, at different temperatures (278.15, 288.15, 298.15, 308.15 and 318.15 K), for 24 hours to reach thermodynamic equilibrium. All experiments were performed at solution pH. The effect of ionic strength was investigated at three levels of NaCl concentration (0.00, 0.01 and 0.10 mol L^{-1}). Blank experiments were carried out using the same experimental procedure without MWCNT to check potential adsorption of dye onto glass tubes. Separation of MWCNT and supernatants was made by centrifugation. The collected aliquots were diluted to ensure that absorbance readings obeyed Beer's Law by UV/Vis spectrophotometry. The amount of adsorbed dye on MWCNT at equilibrium, Γ (mg g^{-1}), was calculated as follows:

$$\Gamma = \left(\frac{C_0 - C_e}{m} \right) V \qquad (1)$$

where Γ is the amount of dye adsorbed onto the MWCNTs (mg g^{-1}) after thermodynamic equilibrium; C_0 and C_e are the initial and the equilibrium concentrations (mg mL^{-1}), respectively; V is the solution volume (mL); and m is the mass of MWCNT used (g).

3. Results and Discussion

3.1. CNT characteristics

The BET surface area, average mesopore and micropore volumes are 188 m^2 g^{-1}, 0.597 cm^3 g^{-1}, and 0.068 cm^3 g^{-1}, respectively. Thermogravimetric analysis, SEM and TEM micrographs are presented in Fig. 2, which shows that MWCNT has purity higher than 90 % and average diameter of 10-40 nm. These data are consistent with the information provided by the supplier of the material, as previously presented.

(a)

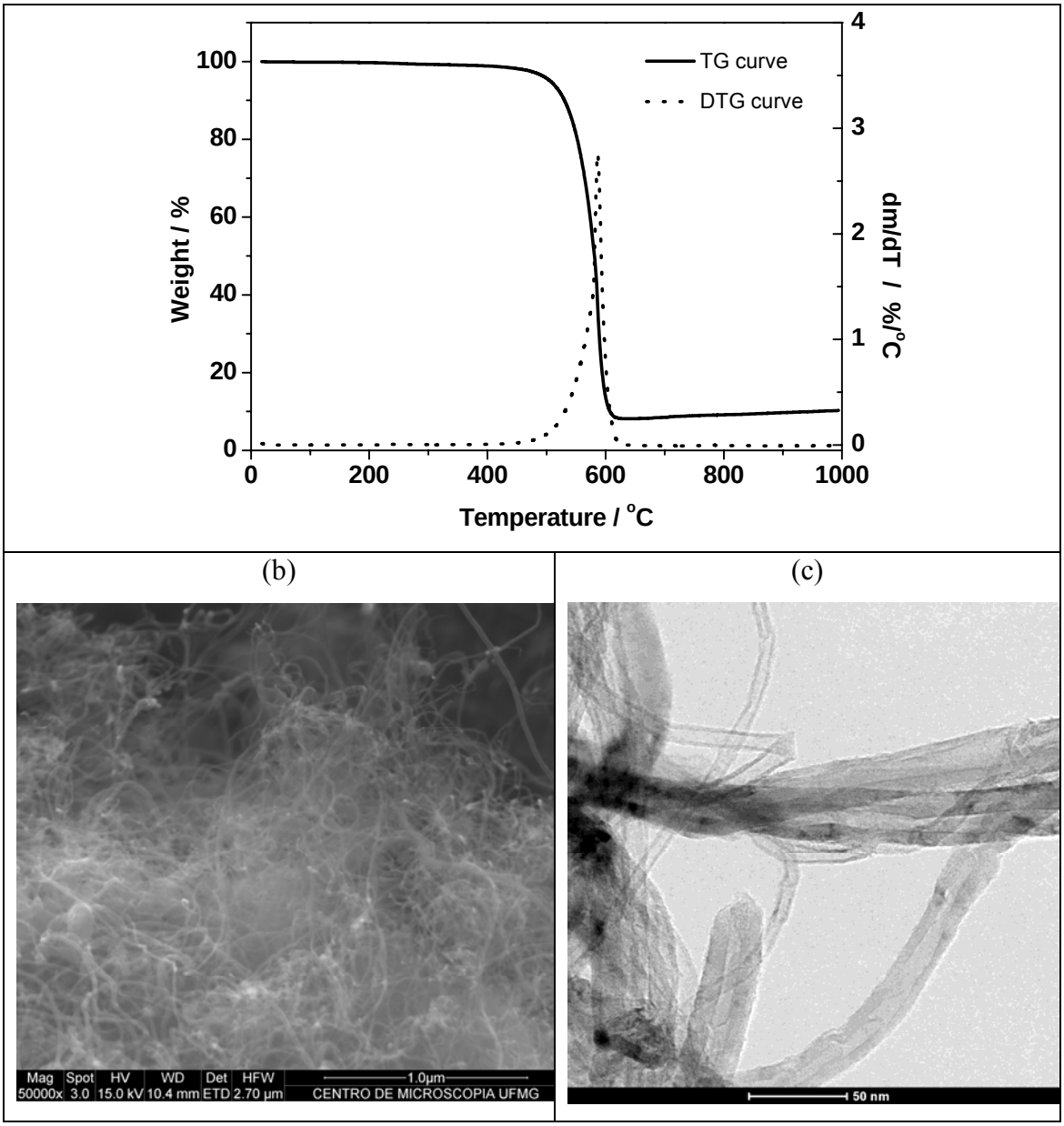

Figure 2. (a) TG e DTG curves, (b) SEM and (c) TEM micrographs.

3.2. Equilibrium study

The adsorption isotherm presents the distribution of adsorbate molecules between the liquid and the solid phases at equilibrium [9]. A period of 24 h was considered to reach thermodynamic equilibrium. In fact, several reports demonstrated that adsorption of dyes onto CNTs takes place until equilibrium in the range of 100-360 min [11-15]. Fig. 3 shows the amounts adsorbed (Γ) of AY, AB and AG plotted against the equilibrium concentrations (C_e) at 298 K.

All isotherms present the same nonlinear profile: an increase in the adsorbed amount with increasing equilibrium concentrations followed by a tendency to form a plateau at

higher concentrations, which describes the maximum adsorption capacity. The order of adsorption follows: AG < AB < AY.

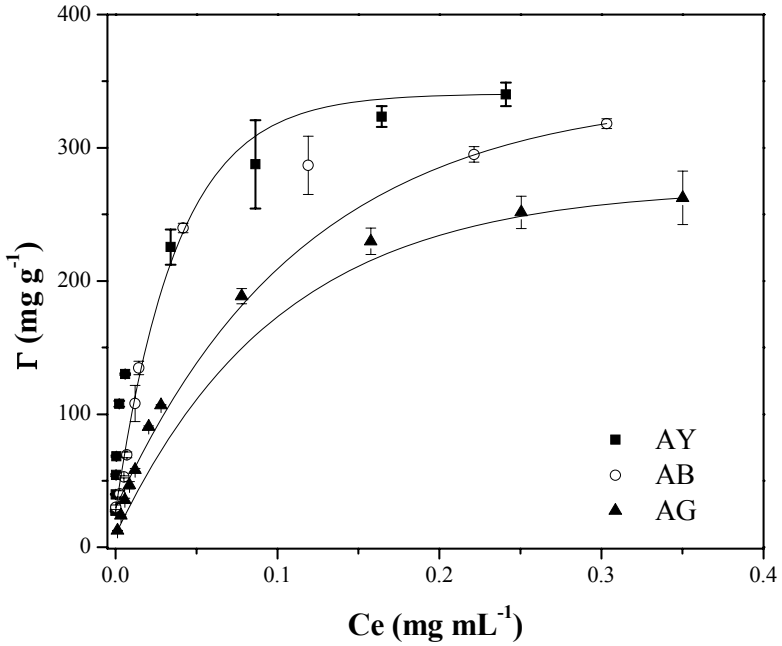

Figure 3. Equilibrium adsorption isotherms of AY, AB and AG onto MWCNT at 298 K.

The Langmuir model is one of the most often used to describe nonlinear experimental data of adsorption isotherms [11,12-15] and was fitted to the experimental data. Langmuir theory proposes that adsorption occurs on a homogeneous surface whose adsorption sites are identical and energetically equivalent. Each surface site adsorbs only one molecule, and the energy is equivalent at all sites for the adsorption of one adsorbent molecule, regardless of the presence or absence of other molecules on contiguous sites. This model proposes that a monolayer of adsorbate molecules forms at the interface and no lateral interaction between these molecules occur. The linear form of the Langmuir isotherm equation is represented by:

$$\Gamma = \frac{\Gamma_{\max} K_L C_e}{1 + K_L C_e} \qquad (2)$$

where C_e is the equilibrium concentration of the dye (mg mL^{-1}), Γ is the amount of dye adsorbed (mg g^{-1}), K_L and Γ_{max} are Langmuir constants related to the affinity of the binding sites (adsorption energy) and maximum monolayer adsorption capacity,

respectively. The value of Γ_{max} specifies the theoretical saturation capacity of the monolayer and demonstrates that further adsorption will contribute to a prohibitive increase in the Gibbs free energy of the interface. Equation 3 shows the linearized form of the Langmuir model:

$$\frac{C_e}{\Gamma} = \frac{1}{\Gamma_{max}} C_e + \frac{1}{K_L \Gamma_{max}} \quad (3)$$

A plot of C_e/Γ versus C_e enables the calculation of K_L and Γ_{max} from the intercept and slope of the data linear regression, respectively. Table 1 shows the values of Langmuir constants calculated from the intercept and slope of the linear plot for each dye on MWCNT.

Table 1. Coefficients of the Langmuir model fitted for AY, AB and AG on MWCNT at 298 K.

Adsorbate	Γ_{max} (mg g^{-1})	K_L (g mg^{-1})	R^2
Acid yellow 42	337.84	190.21	0.99345
Acid black 210	328.95	58.72	0.99002
Acid green 68:1	294.12	23.11	0.99768

All isotherms shown in Fig. 3 confirm the formation of a monolayer coverage, since all data were very well fitted by the Langmuir isotherm model ($R^2 > 0.99$). The constants Γ_{max} and K_L indicate the same tendency demonstrated by the isotherms: AY presents higher adsorption than AB, which, in turn, presents higher adsorption than AG. This order suggests that molecular structure of adsorbates may affect adsorption mechanism.

3.3. Thermodynamic study

Thermodynamic parameters, i.e., the change in Gibbs free energy of adsorption ($\Delta_{ads}G°$), the change in enthalpy of adsorption ($\Delta_{ads}H°$) and the change in entropy of adsorption ($\Delta_{ads}S°$), were estimated to assess the nature of interactions on the adsorption

between azo dyes and CNTs. The Gibbs standard free energy change is related to the equilibrium constant (K°) by the following equation:

$$\Delta_{ads} G^o = -RT \ln K^o \tag{4}$$

where K° is the equilibrium constant of the adsorption process, R is the universal gas constant (8.314 J K^{-1} mol^{-1}), and T is the temperature in Kelvin. The equilibrium constant for the adsorption process, K°, is obtained when $\mu_i^{\text{int}} = \mu_i^{sol}$, and $\mu_i^{sol,or,\text{int}} = \mu_i^o + RT \ln a_i^{sol,or,\text{int}}$, in which μ_i^{int} is the chemical potential of *i* (i.e., the azo dye) adsorbed at the MWCNT–solution interface; μ_i^{sol} is the chemical potential of *i* in solution (at equilibrium); μ_i^o is the chemical potential of *i* at a standard condition; and $a_i^{sol,or,\text{int}}$ is the activity of *i* (in solution or at the MWCNT–solution interface). After some manipulation of the equations, the following relationship is obtained:

$$K^o = \frac{a_i^{\text{int}}}{a_i^{sol}} = \frac{\gamma_i^{\text{int}} C_i^{\text{int}}}{\gamma_i^{sol} C_i^{sol}} \tag{5}$$

where C_i^{int} is the concentration of the adsorbed dye at the MWCNT-solution interface (mg g^{-1}), C_i^{sol}, is the concentration of dye in solution at equilibrium (mg mL^{-1}), γ_i^{int} is the activity coefficient of the adsorbed dye and γ_i^{sol} is the activity coefficient of the dye in solution at equilibrium.

In dilute solutions with low surface coverage, the activity coefficients approach unity, thereby reducing Eq. (5) to:

$$K^o = \frac{C_i^{\text{int}}}{C_i^{sol}} = \frac{\Gamma}{C_e} \tag{6}$$

The values of ln K^o can be obtained by plotting ln(Γ/C_e) *versus* C_e and by extrapolating C_e to zero. A straight line can be fitted to the points based on a least-squares analysis. Its intercept with the vertical axis yields the values of ln K^o that are used in Eq. (4).

It is also known that the Gibbs free energy change is related to the changes in enthalpy and entropy at constant temperature by the following equation:

$$\Delta_{ads} G^o = \Delta_{ads} H^o - T\Delta_{ads} S^o \quad (7)$$

The combination of Eq. (7) and Eq. (4), gives:

$$\ln K^o = -\frac{\Delta_{ads} H^o}{RT} + \frac{\Delta_{ads} S^o}{R} \quad (8)$$

$\Delta_{ads}H°$ and $\Delta_{ads}S°$ can then be calculated from the slope and intercept of the van't Hoff plots of ln K° *versus* 1/T, respectively. Table 2 shows these thermodynamic parameters estimated from the adsorption of AY, AB and AG on MWCNT.

Table 2. Thermodynamic properties obtained by van't Hoff approximation of adsorption of azo dyes on MWCNT.

Dyes	$\Delta_{ads}G°$/ kJ mol^{-1}	$\Delta_{ads}H°$/ kJ mol^{-1}	$T\Delta_{ads}S°$/ kJ mol^{-1}
Acid yellow 42	-31.88	49.86	81.74
Acid black 210	-26.04	69.75	95.79
Acid green 68:1	-20.82	55.76	76.58

The adsorption of azo dyes onto MWCNT is a spontaneous process ($\Delta_{ads}G° < 0$) and thermodynamic favorability follows the order of $\Delta_{ads}G°$: AY > AB > AG.

The values of enthalpy change ($\Delta_{ads}H°$) confirm that the adsorptions of all azo dyes on MWCNT are endothermic phenomena, and further support is given by the increase of adsorption capacity with increasing temperature.

The positive value of $\Delta_{ads}S°$ shows that the driving force of the process is the entropy change, described as the increase in the degrees of freedom at the solid-liquid interface during adsorption of azo dyes onto MWCNT. Desolvation of AY, AB and AG molecules and the MWCNT surface during adsorption may cause this phenomenon, due to the increase in the configurational entropy of water molecules at the liquid bulk phase.

Only a few investigations have reported the interaction of dyes and carbon nanotubes. Yan *et al*. show that methylene blue interacts with the SWCNT through charge-transfer and hydrophobic interactions [23]. Liu *et al*. reported that two main factors have been found to play the key roles for the dye-MWCNT interactions: molecular geometry and charge. It was proposed that molecules with planar structures and higher charge load favored the adsorption [24]. In our work, the thermodynamic properties calculated by van't Hoff approximation show that the interactions presented in the adsorption of azo dyes onto MWCNT may not drive to spontaneity, due to the endothermic nature of the process.

3.4. Effect of ionic strength

Since large amounts of salts are applied in the dyeing process, the effect of ionic strength on the adsorption was evaluated by examining any changes in the isotherms [13,21]. Figures 4a, 4b and 4c present the influence of the ionic strength on the adsorption of acid yellow 42, acid black 210 and acid green 68:1, respectively, at three distinct sodium chloride concentrations.

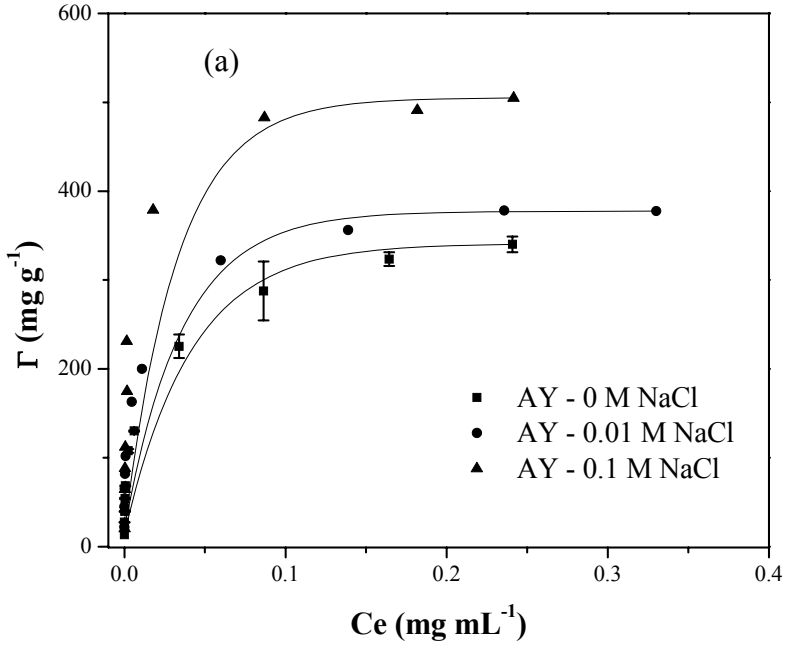

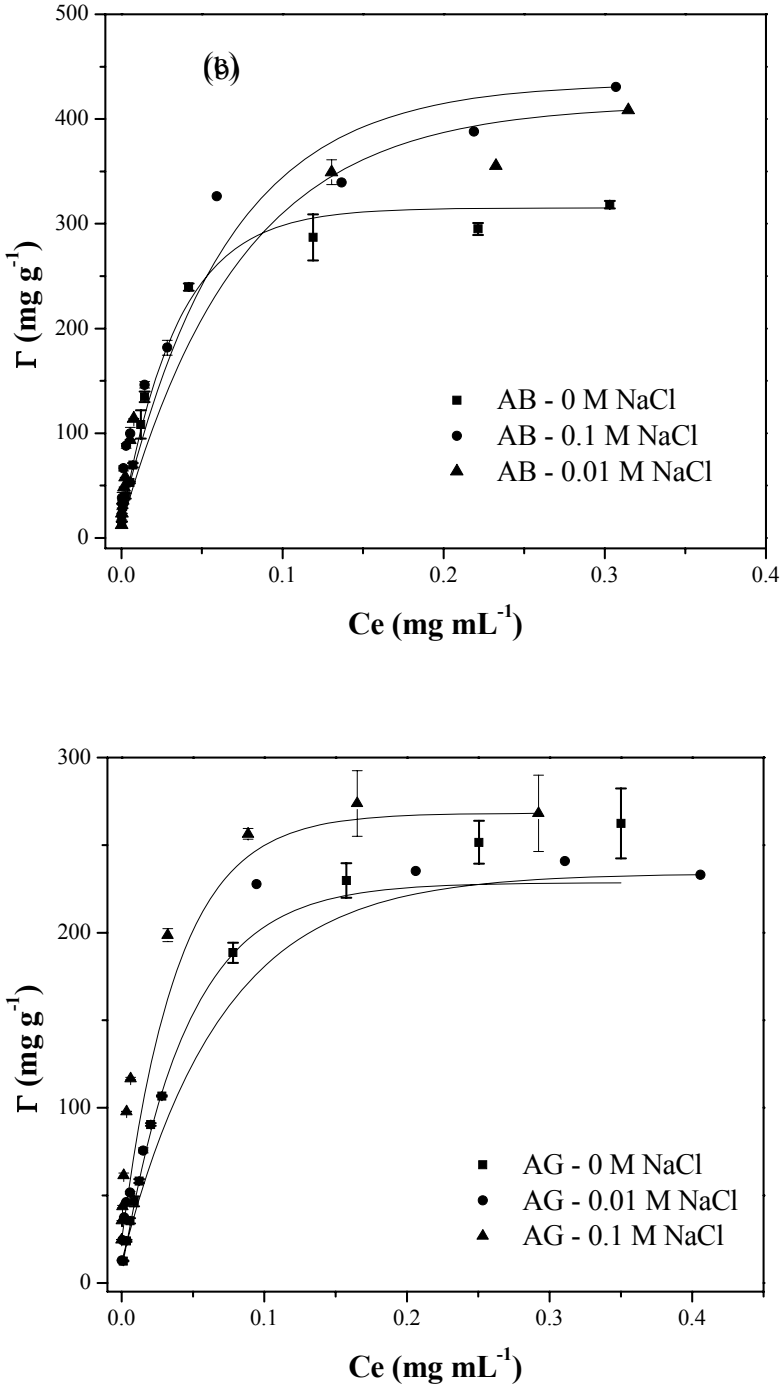

Figure 4. Effect of ionic strength on the adsorption isotherms of AY (a), AB (b) and AG at 298 K.

The increase in ionic strength causes an increase in the amount of adsorption of azo dyes onto MWCNT. The higher adsorption capacity of CNTs upon salt addition can be attributed to the aggregation of dye molecules induced by the action of salt ions, i.e., salt ions force dye molecules to aggregate, increasing the extent of adsorption of dyes

onto CNTs [13]. The adsorption extent of dyes onto the CNT's surface is also dependent of the so-called screening effect – the CNT may be charged on the surface due to the presence of oxygenated groups, being able to reach neutrality by oppositely charged ions from dissolved salt. The latter effect may be validated if the carbon nanotubes present heterogeneous surface.

On the other hand, ionic strength could alter the aggregation state of MWCNT, leading to a better dispersion in the salt solution, when compared with distilled water. This phenomenon could increase the specific surface area, which may contribute to higher amounts of adsorbed dyes per gram of MWCNT.

3.5. Surface modification – equilibrium and thermodynamic studies

Isotherms of adsorption of acid yellow 42 on MWCNT-acid, MWCNT-oxid and pristine MWCNT at 298 K are presented in Fig. 5. The adsorption capacity of the different adsorbents follows the order: MWCNT > MWCNT-oxid > MWCNT-acid, so the surface modification of MWCNT decreased the amount of adsorbed dye in comparison with pristine MWCNT. The order also shows that nitric acid treatment enables a more intense modification of the MWCNT surface than hydrogen peroxide treatment, in comparison with pristine MWCNT.

The decrease in the extent of AY adsorption may be explained by the presence of oxygenated functional groups at the CNTs modified surfaces, which can affect, even minimally, the adsorptive properties of the adsorbent [18]. The surface of pristine CNT is supposed to be more homogeneous, with delocalized π-electrons that enhance the adsorption capability of aromatic compounds, when compared with other carbon-based adsorbents. Several works indicate that the so-called π-π dispersion forces are responsible for the adsorption of aromatic compounds onto CNT [22]. Oxidation may introduce oxygenated functional groups on the CNT surface, thereby creating a hydrophilic environment [14] and inhibiting adsorption of aromatic compounds by π-π dispersion forces [18]. Another explanation is that the adsorption of water molecules occurs on the oxidized sites of the modified CNT by means of hydrogen bonding [20], which is the so-called "solvent effect". In a previous work, we suggested that specific interactions of phenolic molecules (aromatic compounds) with functional groups that are chemisorbed onto the surface of the MWCNTs (probably hydrogen bonds) are the driving force of the adsorption process [26]. Therefore, the solvent effect and the

oxidation of MWCNTs, by the introduction of new functional groups on the adsorbent surface, inhibit the adsorption of azo dyes due to the localization of the π-electron on the adsorbent surface.

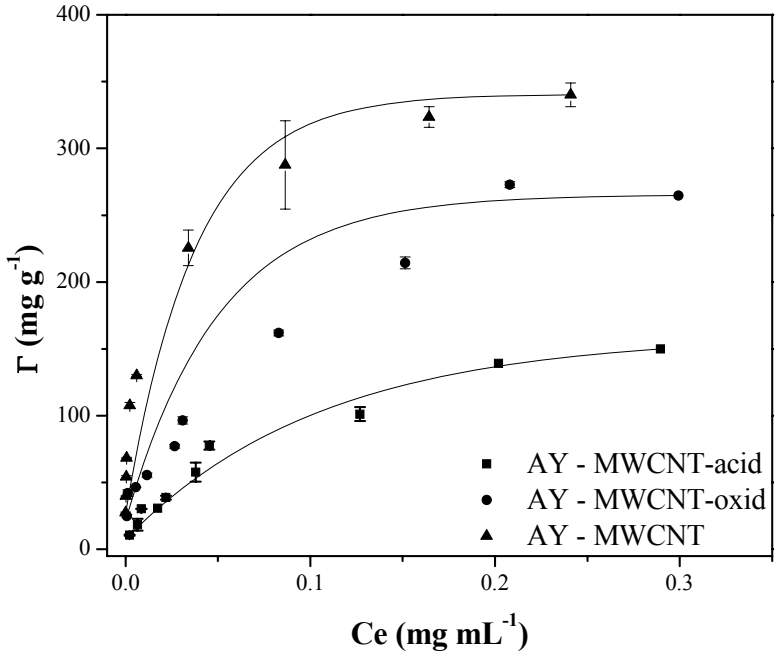

Figure 5. Adsorption isotherms of AY onto MWCNT-acid, MWCNT-oxid and pristine MWCNT at 298 K.

3.5. Microcalorimetry studies

The energy released or absorbed as heat in a thermodynamic process can be measured by equipments and calorimetric techniques that allow their detection. Among these, Isothermal Titration Microcalorimetry (ITC) has been widely used in the characterization of many molecular processes due its high sensitivity, with the possibility of detecting energy flows in the order of 10^{-9} J occurring in a given process.

Curves of variation of the enthalpy of adsorption ($\Delta_{ads}H$) versus the equilibrium concentration of AY, AB and AG on MWCNT obtained from ITC measurements at 298 K are shown in Fig. 6.

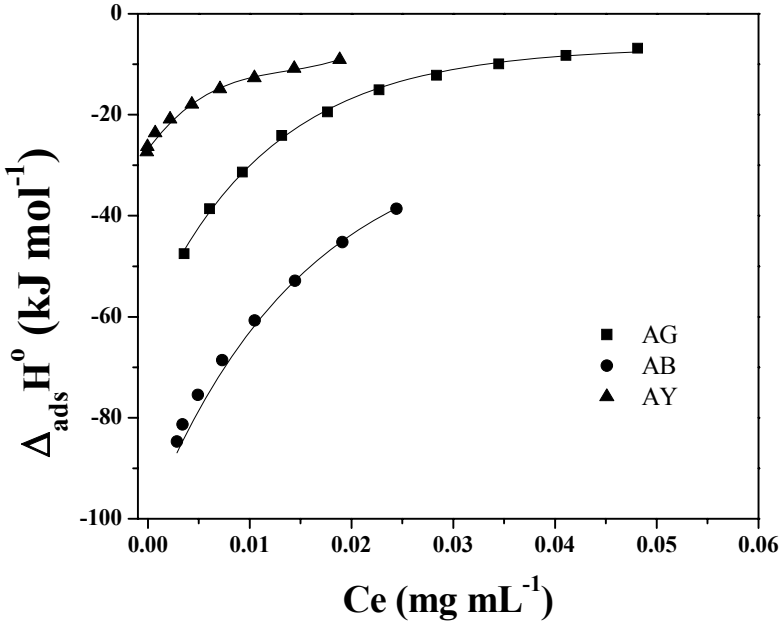

Figure 6. $\Delta_{ads}H$ (kJ mol^{-1}) versus equilibrium concentration (mg mL^{-1}) for the adsorption process of AY, AB and AG on MWCNT.

According to Equation (9), the $\Delta_{ads}H$ values reflect the contributions of five processes: the $\Delta_{deh}H_{AD-H_2O}$ and the $\Delta_{deh}H_{MWCNT-H_2O}$, which are the enthalpy changes of dehydration for the specific azo dye and MWCNT, respectively (both endothermic); the exothermic $\Delta_{int}H_{H_2O-H_2O}$ that is related to the interaction between water molecules released during the desolvation process; $\Delta_{int}H_{AD-AD(MWCNT)}$ (exothermic or endothermic), which describes the interaction energy between molecules of the azo dye adsorbed onto adjacent sites on the MWCNT surface; and the exothermic $\Delta_{int}H_{MWCNT-AD}$, which indicates the intensity of the enthalpic interaction between the dye molecules and the carbon nanotube surface. It is well known that the values of $\Delta_{deh}H_{AD-H_2O}$, $\Delta_{int}H_{AD-AD(MWCNT)}$ and $\Delta_{int}H_{MWCNT-AD}$ differ from one dye compound to another.

$$\Delta_{ads}H = \Delta_{deh}H_{AD-H_2O} + \Delta_{des}H_{MWCNT-H_2O} + \Delta_{int}H_{H_2O-H_2O} + \Delta_{int}H_{AD-AD(MWCNT)} + \Delta_{int}H_{MWCNT-AD} \quad (9)$$

According to Fig. 6, the negative values of $\Delta_{ads}H$ indicate the exothermic nature of

all adsorption processes and, upon each injection, $\Delta_{ads}H$ tends to approach zero at higher levels of the equilibrium concentration of dye. At the beginning of the adsorption process, the amount of energy released as heat ($\Delta_{ads}H$) follows the order: AB > AG > AY. As C_e reaches higher values, the change of enthalpy of adsorption becomes less negative, which confirms the presence of distinct sites on the MWCNT surface that are capable of interacting distinctly with the azo dyes. This evidence shows that the heterogeneity of the MWCNT surface influences the adsorption process, due to electrostatic interactions between the functional groups on the surface and the charged groups of the azo dyes.

Electrostatic interactions and π–π dispersion forces may occur simultaneously, explaining the general mechanism of adsorption, and the balance between them may be modulated by the chemical structure of the azo dye. In fact, Wang *et al*. recently reported that electronic attraction and π–π interaction are involved in dye adsorption, and π–π interaction was the major driving force of the process [25].

Table 3 lists the values of thermodynamic properties obtained by ITC. Contrasting with those estimated by the van't Hoff approximation, the negative values of $\Delta_{ads}H°$ confirm an exothermic process of adsorption. The negative values of $\Delta_{ads}S°$ to AB and AG adsorption indicate a decrease in the entropy change for the adsorbate molecules at the MWCNT-solution interface, caused by a reduction in the configuration entropy of the azo dye molecular structure. Therefore, adsorption of AB and AG onto MWCNT is an enthalpically driven process. On the other hand, the positive value of $\Delta_{ads}S°$ for the adsorption of AY on MWCNT denotes an increase in the entropy change for those molecules at the MWCNT-solution interface, due to the enlargement in the configuration entropy of the dye molecules. In this case, both contributions of enthalpy change and entropy change of adsorption determine the thermodynamic spontaneity of the process.

Table 3. Thermodynamic properties of the adsorption of azo dyes on MWCNT obtained by ITC.

Dyes	$\Delta_{ads}G°$/ kJ mol^{-1}	$\Delta_{ads}H°$/ kJ mol^{-1}	$T\Delta_{ads}S°$/ kJ mol^{-1}
Acid yellow 42	-31.88	-26.87	5.01
Acid black 210	-26.04	-100.06	-74.02
Acid green 68:1	-20.82	-60.70	-39.88

The data in Table 3 also prove that van't Hoff approximation provides an incomplete and erroneous interpretation of the interactions between the azo dyes studied and MWCNTs. The ITC technique seems to present more reliable results. Furthermore, it is suitable to provide a good understanding of the surface chemistry of carbon-based adsorbents, such as carbon nanotubes.

4. Conclusions

This work proposes, for the first time, the use of isothermal titration calorimetry (ITC) to evaluate the surface of a MWCNT sample and the nature of its interactions with azo dyes compounds. The adsorption of acid yellow 42, acid black 210 and acid green 68:1 was evaluated using thermodynamic properties obtained by ITC and van't Hoff approximation. The adsorption of all azo dyes onto MWCNT is spontaneous ($\Delta_{ads}G^{o} < 0$). Adsorptions of AB and AG onto MWCNT are enthalpically driven, while AY is adsorbed by contributions of both enthalpy and entropy changes according to ITC measurements. Calorimetric results show that interactions between azo dyes and MWCNT occur at different sites, and electrostatic interactions and π–π dispersion forces may occur simultaneously, explaining the general mechanism of adsorption. The balance between them may be modulated by the chemical structure of the azo dye.

It has been demonstrated that the Langmuir model provides good fittings to experimental data ($R^2 > 0.99$), although its theoretical background does not explain the results obtained by ITC. The van't Hoff approximation provides an incomplete and erroneous interpretation of the interactions between the azo dyes studied and MWCNTs.

This work also shows, for the first time, that the ITC technique can be applied to describe the surface of a MWCNT sample, and to elucidate its interactions with adsorbed azo dyes molecules.

References

[1] Machado FM, Bergmann CP, Fernandes THM, Lima EC, Royer B, Calvete T, Fagan SB. Adsorption of Reactive Red M-2BE dye from water solutions by multi-walled carbon nanotubes and activated carbon. J Hazard Mater 2011;192(3):1122-31.

[2] Nethaji S, Sivasamy A. Adsorptive removal of an acid dye by lignocellulosic waste biomass activated carbon: Equilibrium and kinetic studies. Chemosphere 2011;82(10):1367-72.
[3] Wang L. Application of activated carbon derived from 'waste' bamboo culms for the adsorption of azo disperse dye: Kinetic, equilibrium and thermodynamic studies. J Environ Manage 2012;102:79-87.
[4] Jiang R, Fu YQ, Zhu HY, Yao J, Xiao L. Removal of methyl orange from aqueous solutions by magnetic maghemite/chitosan nanocomposite films: Adsorption kinetics and equilibrium. J Appl Polym Sci 2012;125:E540-49.
[5] Mahmoodi NM, Najafi F. Preparation of surface modified zinc oxide nanoparticle with high capacity dye removal ability. Mater Res Bull 2012;47:1800-09.
[6] Zahra A, Imran M, Kanwal F. Comparative Adsorption Studies of Methyl Orange Using Different Varieties of Melon Seeds as Adsorbents. Asian J Chem 2012;24(6):2668-70.
[7] Wang F, Li C, Yu JC. Hexagonal tungsten trioxide nanorods as a rapid adsorbent for methylene blue. Sep Purif Technol 2012;91:103-07.
[8] Zhao S, Zhou F, Li L, Cao M, Zuo D, Liu H. Removal of anionic dyes from aqueous solutions by adsorption of chitosan-based semi-IPN hydrogel composites. Composites: Part B-Eng 2012;43(3):1570–78.
[9] Hameed BH, Ahmad AL, Latiff KNA. Adsorption of basic dye (methylene blue) onto activated carbon prepared from rattan sawdust. Dyes Pigments, 2007;75: 143-49.
[10] Mane VS, Mall ID, Srivastava VC. Use of bagasse fly ash as an adsorbent for the removal of brilliant green dye from aqueous solution. Dyes Pigments, 2007;73:269-78.
[11] Yao Y, Xu F, Chen M, Xu Z, Zhu Z. Adsorption behavior of methylene blue on carbon nanotubes. Bioresource Technol, 2010;101:3040–46.
[12] Gong JL, Wang B, Zeng GM, Yang CP, Niu CG, Niu QY, ZhouWJ, Liang Y. Removal of cationic dyes from aqueous solution using magnetic multi-wall carbon nanotube nanocomposite as adsorbent. J Hazard Mater, 2009;164: 1517–22.
[13] Kuo CY, Wu CH, Wu JY. Adsorption of direct dyes from aqueous solutions by carbon nanotubes: Determination of equilibrium, kinetics and thermodynamics parameters. J Colloid and Interf Sci, 2008;327:308–15.
[14] Mishra AK, Arockiadoss T, Ramaprabhu S. Study of removal of azo dye by functionalized multi walled carbon nanotubes. Chem Eng J, 2010;162:1026–34.
[15] Wu CH. Adsorption of reactive dye onto carbon nanotubes: Equilibrium, kinetics and thermodynamics. J Hazard Mater, 2007;144: 93–100.

[16] Shapour R, Mehrorang G, Kianoosh M. Multiwalled carbon nanotubes as efficient adsorbent for the removal of congo red. Fresen Environ Bull, 2011;20(10): 2514-20.
[17] El-Sheikh AH. Effect of oxidation of activated carbon on its enrichment efficiency of metal ions: Comparison with oxidized and non-oxidized multi-walled carbon nanotubes. Talanta, 2008;75: 127–34.
[18] Salam MA, Burk RC. Thermodynamics of pentachlorophenol adsorption from aqueous solutions by oxidized multi-walled carbon nanotubes. Appl Surf Sci, 2008;255:1975–81.
[19] Christensen JJ; Hansen LD, Izatt RM. Handbook of proton ionization heats and related thermodynamic quantities; New York: John Wiley and Sons; 1976.
[20] Dąbrowski A, Podkościelny P, Hubicki Z, Barczak M. Adsorption of phenolic compounds by activated carbon—a critical review. Chemosphere, 2005;58: 1049–70.
[21] Liao P, Malik I Z, Zhang W, Yuan S, Tong M, Wang K, Bao, J. Adsorption of dyes from aqueous solutions by microwave modified bamboo charcoal. Chemical Engineering Journal, 195-196, 339–346, 2012.
[22] Lin D, Xing B. Adsorption of phenolic compounds by carbon nanotubes: role of aromaticity and substitution of hydroxyl groups, Environ. Sci. Technol., 2008;42: 7254-59.
[23] Yan Y, Zhang M, Gong K, Su L, Guo Z, Mao L. Adsorption of Methylene Blue Dye onto Carbon Nanotubes : A Route to an electrochemically functional nanostructure and its layer-by-layer assembled nanocomposite, Chem. Mater., 2005;17: 3457–3463.
[24] Liu CH, Li JJ, Zhang HL, Li BR, Guo Y. Structure dependent interaction between organic dyes and carbon nanotubes, Colloid. Surf. A, 2008;313: 9–12.
[25] Wang S, Ng CW, Wang W, Li Q, Hao Z. Synergistic and competitive adsorption of organic dyes on multiwalled carbon nanotubes. Chem. Eng. J., 2012;197: 34–40.
[26] R.L. Lavall, C.R. Oliveira, A.B. Mageste, M.C.H. da Silva, L.H.M. da Silva. Adsorção de compostos fenólicos em nanotubos de carbono de paredes múltiplas: uma abordagem termodinâmica. Proceedings of the 34ª Reunião Anual da Sociedade Brasileira de Química; 2012 May 23-26; Florianóplis, Brazil.